Analytical solution for the dynamic study of non-uniform cylindrical piles with generalized end conditions in non-homogeneous elastic soil

Andrés Felipe Córdoba Ordoñez

Universidad Nacional de Colombia
Facultad de Minas, Departamento de Ing. Civil
Medellín, Colombia
2023

Analytical solution for the dynamic study of non-uniform cylindrical piles with generalized end conditions in non-homogeneous elastic soil

Andrés Felipe Córdoba Ordoñez

Dissertation for the degree of:
Master of Geotechnical Engineering

Advisor:
Ph.D., David Guillermo Zapata Medina
Co-advisor:
Ph.D., Carlos Alberto Vega Posada

Research line:
Soil-Structure Interaction

Universidad Nacional de Colombia
Facultad de Minas, Departamento de Ing. Civil
Medellín, Colombia
2023

Dedicatory

"If I have seen further, it is by standing on the shoulders of giants"

Isaac Newton.

In memory of Nieves Inés Urbano, the kindest person I have ever known.

Acknowledgements

To my parents, I want to express my heartfelt gratitude for their love, support, patience, and for making my dreams come true. All that I am is thanks to them. I cannot adequately express how much I love them.

To my professors, David Zapata and Carlos Vega, I extend my sincerest gratitude for their unwavering support and invaluable guidance throughout the course of this research. Their expertise and advice have been instrumental in its development.

To Maria de los Angeles Clariet Meza Abalo and Jorge Eliecer Ballesteros Ortega, I would like to express my sincere appreciation for their unwavering support in this project. Their assistance and encouragement have been invaluable.

Finally, I am profoundly grateful to the Universidad Nacional de Colombia for enabling my master's studies. Its exceptional education, abundant resources, and unwavering support have not only shaped my academic journey but also instilled in me a profound sense of gratitude. I truly appreciate the university's unwavering belief in my potential to succeed in my chosen field.

Abstract

This paper presents a simplified analytical method for the dynamic study of non-uniform cylindrical piles with generalized end conditions in non-homogeneous elastic soil. The governing differential equation (GDE) of the proposed element is derived in a classical way by using Timoshenko approach and solved using the Differential Transformation Method (DTM). This complex analysis is reduced to solve a system of two linear algebraic equations, which solution is readily available and easy to code. The proposed model represent a general solution capable to solve, just by using a single segment per element, the static, dynamic and stability analyses. The proposed model includes the frequency effects on the stiffness matrix and load vector as well as the coupling effects of: (i) bending and shear deformations along the member; (ii) translational and rotational masses uniformly distributed along its span; (iii) axial load (tension or compression) applied at both ends; (iv) shear forces along the span induced by the applied axial load as the beam deforms according to the "modified shear equation" proposed by Timoshenko; (v) generalize boundary condition at the ends of the element (i.e., translational and rotational constraints) and (vi) two-parameter elastic foundations. The dynamic analyses of framed structures can be performed by including the effects of the imposed frequency ($\omega > 0$) on the dynamic-stiffness matrix and load vector while the static and stability analyses can be carried out by making the frequency ($\omega = 0$). Analytical results indicate that the elastic behavior of non-uniform cylindrical piles is frequency dependent and highly sensitive to the coupling effects mentioned above.

Keywords: Non-uniform cylindrical pile; Tapered Timoshenko beam; Semi-rigid connection; Non-homogeneous soil; Partially embedded pile; Dynamic response; Differential Transformation Method.

Resumen

Solución analítica para el estudio dinámico de pilotes cilíndricos no uniformes con condiciones de borde generalizadas en suelos elásticos no homogéneos

Este documento presenta un método analítico simplificado para el estudio dinámico de pilotes cilíndricos no uniformes con condiciones de borde generalizadas en suelo elástico no homogéneo. La ecuación diferencial gobernante (EDG) del elemento propuesto se deriva de manera clásica utilizando el enfoque de Timoshenko y se resuelve utilizando el Método de Transformada Diferencial (DTM). Este análisis complejo se reduce a resolver un sistema de dos ecuaciones lineales algebraicas, cuya solución está disponible y es fácil de codificar. El modelo propuesto representa una solución general capaz de resolver, utilizando solo un segmento por elemento, los análisis estáticos, dinámicos y de estabilidad. El modelo propuesto incluye los efectos de frecuencia en la matriz de rigidez y el vector de carga, así como los

efectos de acoplamiento de: (i) deformaciones por flexión y corte a lo largo del elemento; (ii) masas de translación y rotación distribuidas uniformemente a lo largo de su longitud; (iii) carga axial (tensión o compresión) aplicada en ambos extremos; y (iv) fuerzas de corte a lo largo de la longitud inducidas por la carga axial aplicada, a medida que la viga se deforma según la "ecuación de corte modificada"propuesta por Timoshenko, (v) condiciónes de borde generalizadas, (vi) fundaciones elásticas de dos parámetros. Los análisis dinámicos de estructuras con marcos se pueden realizar incluyendo los efectos de la frecuencia impuesta ($\omega > 0$) en la matriz de rigidez dinámica y el vector de carga, mientras que los análisis estáticos y de estabilidad se pueden realizar haciendo que la frecuencia ($\omega = 0$). Los resultados analíticos indican que el comportamiento elástico de pilas cilindrcas con seccion no uniforme dependen de la frecuencia impuesta y es altamente sensible a los efectos de acoplamiento mencionados anteriormente.

Palabras clave: Pila cilindrica no prismática; Viga Timoshenko acartelada; Conexión semirigida; Suelo no homogéneo; Pila parcialmente embebida; Respuesta dinamica; Metodo de la transformada diferecial.

Content

Nomenclature

Symbol	Definition
$A(x)$	gross sectional area of the beam column
A_s	effective area for shear of the beam-column ($= A(x)/n$)
C_1, C_2, C_3, C_4	constants according to boundary conditions
E	elastic modulus of the material
$\{F_{FE}\}$	loading vector, fixed-end forces and moments in member AB
	due to external applied load
G	shear modulus of the material
I	moment of inertia of the beam-column cross section
$\bar{J}(k)$	differential transform of the function $\bar{Y}(\xi)$
J_a and J_b	rotational inertia of the concentrated masses at A and B, respectively
κ_s	first parameter of elastic foundation
κ_G	second parameter of elastic foundation
K_o	Modulus of subgrade reaction at coordinate $x = 0$
$[K]$	dynamic-stiffness matrix of the beam-column
L	beam-column span
$\bar{m}$	mass per unit length of the beam-column at A
M	bending moment
$\bar{M}(\xi)$	bending moment parameter (dimensionless)
m_h	slope of the soil variation
n	effective shear factor of the beam-column cross section
P	compression or tension axial load applied at the ends of the beam-column
$q(x,t)$	applied transverse load
r	radius of gyration of the beam cross section
r_b	radius at bottom of the pile

Symbol	Definition
r_t	radius at top of the pile
R	slenderness parameter ($= r/L$)
R_a and R_b	stiffness indices of the flexural connections at A and B, respectively
S_a and S_b	stiffness of the lateral bracing at ends A and B of the beam-column, respectively
t	time
$\{U\}$	vector of displacements and rotations
V	shear force
$\bar{V}(\xi)$	dimensionless shear force
x	coordinate along the centroidal axis of the beam-column
y	total lateral deflection of the centroidal axis of the beam-column
$Y(x)$	shape-function of the total lateral deflection of the centroidal axis of the beam-column
$\bar{Y}(\xi)$	dimensionless shape-function of the total lateral deflection of the centroidal axis of the beam-column
γ_s	shear distortion
$\frac{\partial^2 y}{\partial t^2}$	lateral acceleration of the centroidal axis of the beam-column
$\frac{\partial^2 \theta}{\partial t^2}$	angular acceleration of the centroidal axis of the beam-column
θ	slope due to bending of the centroidal line of the beam-column
$\Theta(\xi)$	shape-function of the slope of the centroidal axis of the beam-column
$\bar{\Theta}(k)$	differential transform of the function $\Theta(\xi)$ due to bending only
κ_a and κ_b	stiffness of the flexural connections at A and B, respectively (force x distance)
ν	Poisson ratio
ρ	mass per unit volume
ρ_a and ρ_b	fixity factors at ends A and B of the beam-column, respectively
ω	circular frequency

1. Introduction

1.1. Background

Foundations play a crucial role in supporting structures and transmitting their loads to the soil, making it important to consider an adequate supporting depth in footing design to prevent lifting, structural damage due to natural phenomena, as well as damage to adjacent structures. In addition, engineers must consider seismic loads, soil capacity, and possible tolerable settlement to avoid ground failure [18]. When the superficial soil layers are too compressible or their bearing capacity is insufficient, it becomes necessary to use deep foundation elements like piles and drilled shafts to support structures in deeper competent soil [16]. Piles are structural members with a small cross-sectional area compared to their length, and their axial capacity is larger than their lateral capacity. While these structural members are typically built with uniform cross-sectional areas, piles with non-prismatic cross-sections have been successfully used in a range of structures, including highways bridges, medium to high-rise buildings, and aircraft structures. By employing a larger cross-section at the pile head than at the tip, weight and strength can be optimally distributed, which sometimes satisfies architectural and functional requirements [1, 11] and provide higher axial capacities than those of straight-sided piles (i.e., assuming the same length and same equivalent volume) [17]. Furthermore, the incorporation of piles with variable cross-sections not only enhances the stability of structures but also yields cost savings through their improved material usage efficiency. It is important to note, however, that utilizing such piles necessitates a more intricate and comprehensive analysis and design process compared to uniform elements. [1, 13].

Numerous research studies have concentrated on study static, dynamic, and stability analyses of framed structures made up of beams and beam-columns under any load conditions. In the case of beam-columns situated on elastic soil, certain scenarios have been specifically addressed using methods tailored for such problems but limited to specific cases. These analyses are treated in many textbooks, for instance, Timoshenko [21, 20] was the first to analyze the simultaneous coupling effects between bending and shear deformations, and between translational and rotational inertia in beams. Numerous studies have been carried out to investigate these coupling effects. Cheng [5], for example, studied extensively the Timoshenko beam using continuous models and matrix methods. Cheng and Pantelides [6] developed the dynamic matrix of the Timoshenko beam with applications to plane frames. Arboleda-Monsalve et al. [2] presented a general matrix approach and load vector by which the static and dyna-

mic response of framed structures made up of beam-columns with any end conditions and supported on two-parameters elastic soils can be determined directly. Aristizabal-Ochoa [4] presented the complete free vibration analysis of the Timoshenko beam-column with generalized end conditions including the phenomenon of inversion of vibration modes (i.e. higher modes crossing lower modes) in shear beams with pinned-free and free-free end conditions, and also the phenomenon of double frequencies at certain values of beam slenderness (L/r). Palacio-Betancur and Aristizabal-Ochoa [15] developed an approach, based on the conjugate beam theory, to determine the static and dynamic response of non-prismatic elements on Pasternak foundation. Here, the soil was considered homogeneous.

The aim of this research is to develop a new analytical solution for dynamic analysis of non-uniform cylindrical piles with generalized end conditions partially and fully embedded in non-homogeneous elastic soil. The proposed approach is based on the well-established differential transformation method (DTM) and offers the advantage of conveniently incorporating the influence of the soil's second parameter, as well as the effects of semi-rigid connections and lateral transverse constraints, on the natural frequency response of the pile, by employing the proposed formulation, the complex analysis of this problem is simplified to solve a system consisting of two linear algebraic expressions. To demonstrate the capabilities of the proposed method, numerical results are presented and compared with other analytical approaches and validate by using finite element analysis by means of the FE software SAP2000. These comparisons serve to highlight the effectiveness and advantages of the new solution.

1.2. Objectives of the research

1.2.1. General objective

Derive an analytical solution for the dynamic study of non-uniform cylindrical piles with generalized end conditions in non-homogeneous elastic soil.

1.2.2. Specific objectives

- Define a structural model and governing equations that represent the soil-structure interaction of cylindrical piles with a non-uniform cross-section embedded on non-homogeneous soil conditions.
- Implement the differential transformation method on the solution of the governing equations.
- Derive the dynamic stiffness matrix of the proposed element to extend the solution to the analysis of fully embedded circular piles with a non-uniform cross-section in multi-layered soils.

1.3. Content of thesis

This research is divided into six chapters as follows:

Chapter 1 provides a state-of-the-art review trough technical and research background of non-prismatic piles and its behavior under static and dynamic stability analysis, as well as its comparison with prismatic piles. Different approaches and methodologies to consider multi-layered and non-homogeneous soils and partially and fully-embedded elements are presented.

In Chapter 2, the analysis procedure is presented, encompassing the structural model, formulation of the governing equation, general solution, and consideration of boundary conditions. This comprehensive approach provides a solid foundation for the subsequent analysis and allows for a thorough examination of the system under study.

In Chapter 3, the assumptions and procedures for solving the differential equations using the Differential Transform Method (DTM) are presented. The chapter also outlines the process of deriving the stiffness matrix and load vector from the analytical solution. Additionally, the equations for computing deflections, rotations, shear, and bending moment along the member are provided, offering a comprehensive understanding of the structural response.

In Chapter 4, the proposed methodology is thoroughly evaluated and validated through four examples. These examples demonstrate the impact of soil non-homogeneity and stiffness variation in soil layers on the lateral deformations of fully and partially embedded prismatic and tapered piles. The evaluation covers various aspects, including deflection, rotation, natural frequency, and buckling loads. By examining these cases, the effectiveness and reliability of the methodology are demonstrated, providing valuable insights into the behavior of the analyzed pile structures.

Chapter 5 summarizes this work and presents conclusions and recommendations.

2. Analysis procedure

2.1. Model Considerations

The proposed beam-column model is an extension of that presented by Meza-Abalo [14] including the effects of a two-parameters elastic foundations considered as a Pasternak foundation with a uniform (i.e., homogeneous soil), linear or trapezoidal (i.e., non-homogeneous soil) variation of the first-parameter, κ_s. The non-homogeneity of the soil is taken into account by assuming a soil distribution equal to $\kappa_s = (\kappa_o + m_h x)$ as presented by [26]. $m_h = 0$ represents a uniform soil with depth; meanwhile, a value of $m_h \neq 0$ represents a linear or trapezoidal distribution, and an applied external transverse load $q(x,t)$ as shown in Fig.**2-1**. The element is made of the beam-column itself AB, the end flexural connections κ_a and κ_b (whose dimensions are given in force-distance/radian), and the lateral springs or bracing S_a and S_b (whose dimensions are given in force/distance) at A and B respectively. For convenience the two following terms ρ_a and ρ_b [3] denoted as the fixity factors at A and B, respectively , are utilized: $\rho_a = 1/(1 + (3EI/L)/\kappa_a)$, and $\rho_a = 1/(1 + (3EI/L)/\kappa_a)$.

It is assumed that beam-column AB: (1) the pile has a diameter $B(x)$, cross-sectional area $A(x)$, second moment of inertia, $I(x)$, and is made up of an elastic and isotropic material with Young's modulus E and shear modulus G; (2) its centroidal axis is a straight line; (3) is loaded axially at the ends along its centroidal axis x with a constant load P, and transversely along the span with an applied external transverse load q(x,t); (4) its transverse sections is circular, with a effective shear area $A_s = kA(x)$; (5) has uniform mass per unit volume ρ; (6) all transverse deflections, rotations, and strains along the beam are small so the principle of superposition is applicable.

On top of that, the pile geometry is denoted as shown in by top (r_t) and bottom radius (r_b), and their relationship by the taper ratio $m = r_b/r_t$ with $0 \leq m \leq 1$. Then, considering an equivalent radius at $L/2$ as $r_{eq} = r_t/2(m+1)$ the variation of the radius, diameter, area and moment of inertia can be expressed as follows:

$$r_x = r_t \left[1 + (m-1)\frac{x}{L}\right] \tag{2-1}$$

$$\phi(x) = B_x = 2r_x \tag{2-2}$$

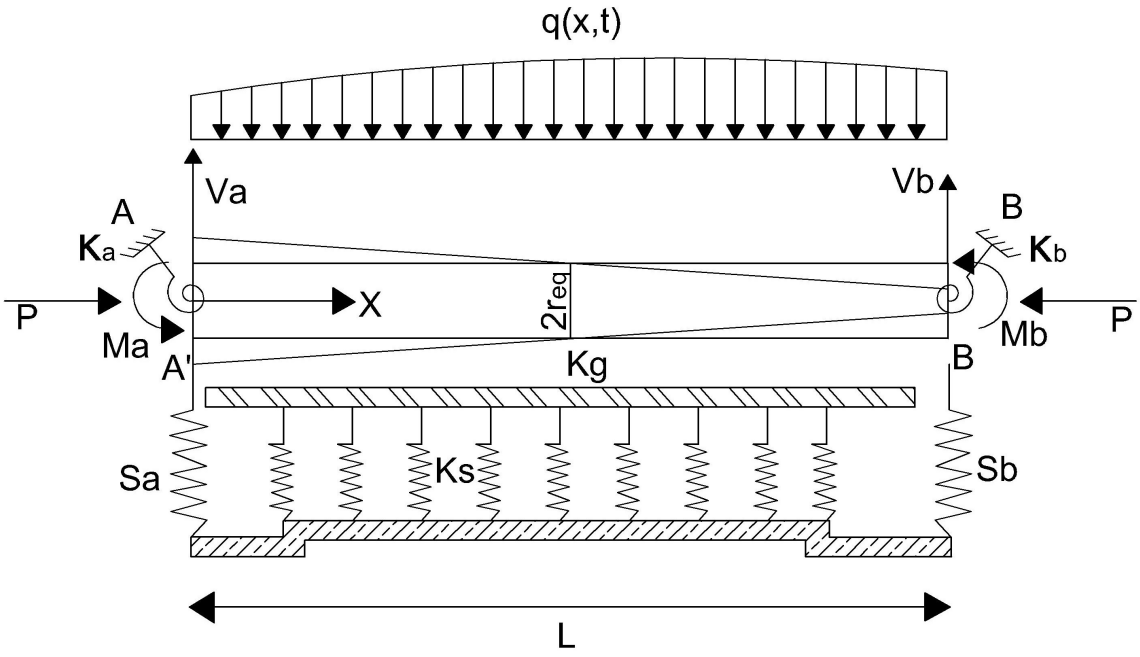

Figure 2-1.: Structural model for beam-column element.

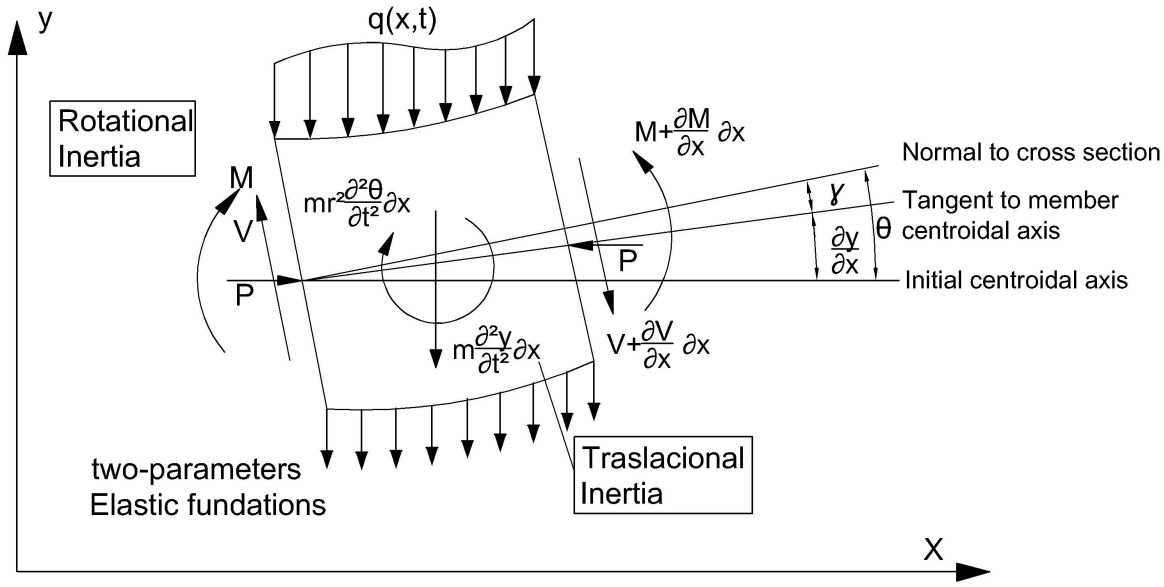

Figure 2-2.: Forces, moments, and deformations on the differential element.

$$A(x) = \pi r_t^2 \left[1 + \frac{x}{L}(m-1)\right]^2 \tag{2-3}$$

$$I(x) = \frac{\pi r_t^4}{4} \left[1 + \frac{x}{L}(m-1)\right]^4 \tag{2-4}$$

2.2. Governing equations and general solution

The governing differential equation of the embedded pile described above Fig. **2-1** is obtained by applying equilibrium to the differential element shown in Fig. **2-2**. The transverse and rotational equilibrium equations are:

$$\frac{\partial V}{\partial x} = -\bar{m}\frac{\partial^2 y}{\partial t^2} - k_s y + k_G \frac{\partial^2 y}{\partial x^2} - q(x,t) \tag{2-5}$$

and

$$\frac{\partial M}{\partial x} = V + \bar{m} r^2 \frac{\partial^2 y}{\partial t^2} - P\frac{\partial y}{\partial x} \tag{2-6}$$

Where $q(x,t) = \gamma_1 + S_1 x + t_1 x^2$ is the quadratic function that describes the distributed load along the member's span; $p(x) = \kappa_s(x) y - \kappa_G y''(x)$ represents the Pasternak soil foundation, here $\kappa_s(x) = (\kappa_o + m_h x)\phi(x)$ and κ_G are the variation of the modulus of sub-grade reaction and shear layer accounting for the interaction of the springs at the top ends, respectively. From Fig. **2-2**, the shear distortion can be expressed as:

$$\gamma_s = \theta - \frac{\partial y}{\partial x} \tag{2-7}$$

According to the *"modified shear approach"* proposed by Timoshenko and Gere [19], the applied axial force P induces a shear component equal to $P\sin\theta \approx P\theta$. Thus, the total shear across the section becomes $V - P\theta$. Thus, the shear force is

$$V = A_s(x)\, G \left(\theta - \frac{\partial y}{\partial x}\right) + P\theta \tag{2-8}$$

and the moment-curvature relationship of the element's cross section is:

$$M = EI(x)\frac{\partial \theta}{dx} \tag{2-9}$$

Substituting Eqs. (2-8) and (2-9) into Eqs. (2-5) and (2-6),

$$A_s(x)\, G \left(\frac{\partial \theta}{\partial x} - \frac{\partial^2 y}{\partial x^2}\right) + A_s'(x)\, G \left(\theta - \frac{\partial y}{\partial x}\right) + P\frac{\partial \theta}{\partial x} = -\bar{m}\frac{\partial^2 y}{\partial t^2} - k_s y + k_G \frac{\partial^2 y}{\partial x^2} - q(x,t) \tag{2-10}$$

$$EI\left(x\right)\frac{\partial^2\theta}{\partial x^2}+EI'\left(x\right)\frac{\partial\theta}{\partial x}=A_s\left(x\right)G\left(\theta-\frac{\partial y}{\partial x}\right)+P\theta+\bar{m}r^2\frac{\partial^2 y}{\partial t^2}-P\frac{\partial y}{\partial x} \tag{2-11}$$

Applying separation of variables to the functions $y(x,t)$, $\theta(x,y)$, and $q(x,y)$, where *"ω"* represents the angular frequency of the oscillating force, involves breaking down these functions into individual components based on their spatial and temporal dependencies:

$$y\left(x,t\right)=Y\left(x\right)\sin\left(\omega t\right), \tag{2-12}$$

$$\theta\left(x,t\right)=\Theta\left(x\right)\sin\left(\omega t\right), \tag{2-13}$$

$$q\left(x,t\right)=Q\left(x\right)\sin\left(\omega t\right) \tag{2-14}$$

By applying separation of variables to the Eqs. (2-10) and (2-11), and recognizing that the temporal dependence $\sin\left(\omega t\right)$ is present in all terms of the function and thus cancels out, the following expressions are obtained:

$$\begin{aligned}&\left(A_s\left(x\right)G+P\right)\frac{d\Theta}{dx}+A_s'\left(x\right)\Theta-\left(A_s\left(x\right)G+k_G\right)\frac{d^2Y}{dx^2}-A_s'\frac{dY}{dx}\\&+\left(k_s-\bar{m}\omega^2\right)Y+Q\left(x\right)=0\end{aligned} \tag{2-15}$$

$$EI\left(x\right)\frac{d^2\Theta}{dx^2}+EI'\left(x\right)\frac{d\Theta}{dx}-\left(A_s\left(x\right)G+P-\bar{m}r^2\omega^2\right)\Theta+\left(A_s\left(x\right)G+P\right)\frac{dY}{dx}=0 \tag{2-16}$$

Eqs. (2-15) and (2-16) represent the vertical and rotational dynamic equilibrium of the beam-column shown in Fig. **2-1**. These equations, which govern the elastic dynamic behavior of the beam-column, are second-order coupled differential equations in Y and Θ.

To facility the static and dynamic analyses of Timoshenko beam-columns supported on two-parameters elastic foundations are reduced in dimensionless parameters presented in Table **2-1** , and are introduced into Eqs.(2-15) and (2-16), along with the terms $\xi=x/L$ and $\bar{Y}=Y/L$.

$$\begin{aligned}&\left(A_\xi+F^2s^2\right)\frac{d\Theta}{d\xi}+A_\xi'\Theta-\left(A_\xi+D_G^2s^2\right)\frac{d^2\bar{Y}}{d\xi^2}-A_\xi'\frac{d\bar{Y}}{d\xi}\\&+\left(D_s^2\left(\xi\right)s^2-b^2s^2nA_\xi\right)\bar{Y}+\frac{L}{A_s(0)G}Q\left(\xi\right)=0,\end{aligned} \tag{2-17}$$

$$s^2I_\xi\frac{d^2\Theta}{d\xi^2}+s^2I_\xi'\frac{d\Theta}{\xi}-\left(A_\xi+F^2s^2-b^2s^2R^2I_\xi\right)\Theta+\left(A_\xi+F^2s^2\right)\frac{d\bar{Y}}{d\xi}=0, \tag{2-18}$$

Table 2-1.: Dimensionless parameters

Parameter	**Description**
$b^2 = \frac{\bar{m}\omega^2}{EI(0)/L^4}$	Frequency parameter
$s^2 = \frac{EI(0)/L^2}{A_s(0)G}$	Bending-to-shear stiffness parameter
$F^2 = \frac{P}{EI(0)/L^2}$	Axial-load parameter
$R^2 = \frac{r(0)^2}{(2L)^2}$	Slenderness parameter
$D_G^2 = \frac{k_G^2}{EI(0)/L^2}$	second parameter of elastic foundation
$Q(\xi) = r_1 + s_1 L\xi + t_1 L^2\xi^2$	Applied transverse load parameter
$\bar{V}_a = \frac{V_a}{A_s(0)G}$ and $\bar{V}_b = \frac{V_b}{A_s(1)G}$	End-shear parameter
$\bar{M}_a = \frac{M_a}{EI(0)/L}$ and $\bar{M}_b = \frac{M_b}{EI(1)/L}$	End bending moment parameter
$R_a = \frac{k_a}{EI(0)/L}$ and $R_b = \frac{k_b}{EI(1)/L}$	End flexural connections indices
$\bar{S}_a = \frac{S_a}{A_s(0)G/L}$ and $\bar{S}_b = \frac{S_b}{A_s(1)G/L}$	End bracing indices
$D_s(\xi) = D_0 + D_1\xi + D_2\xi^2$	first parameter of elastic foundation
$D_0 = \frac{2r_x(0)k_0}{EI(0)/L^4}$	Modulus of sub-grade reaction at coordinate x=0
$D_1 = \frac{2r_x(0)(k_0(m-1)+m_h L)}{EI(0)/L^4}$	Variation of sub-grade soil reaction
$D_2 = \frac{2r_x(0)m_h(m-1)}{EI(0)/L^5}$	Rate at which k_0 increases or decrease along element

Where:

$$I(\xi) = \frac{\pi r_t^4}{4}(1 + (m-1)\xi)^4 = I(0)I_\xi, \tag{2-19}$$

$$A(\xi) = \pi r_t^2(1 + (m-1)\xi)^2 = A(0)A_\xi \tag{2-20}$$

$$Q(\xi) = r_1 + s_1 L\xi + t_1 L^2\xi^2 \tag{2-21}$$

2.3. Shears, moments, deflections and rotations at the ends

In order to determine the stiffness matrix and load vector, the conditions at ends A and B of the beam-column are evaluate following the sign convention for forces, moments, rotations

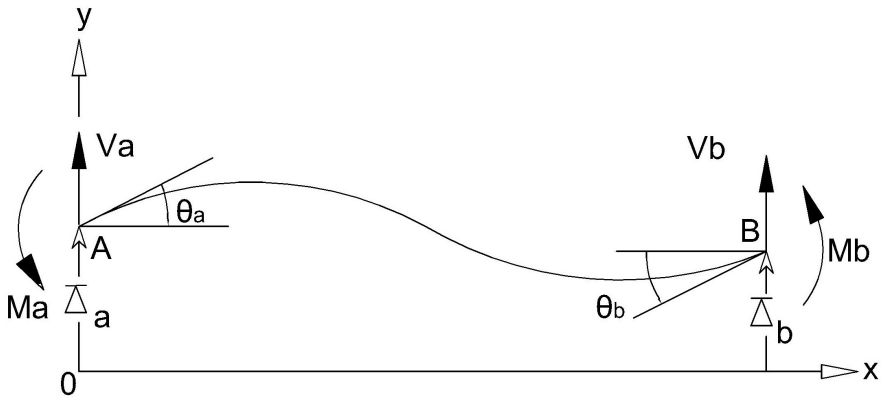

Figure 2-3.: Sign convention (deflections, rotations, shear forces and moments) [2].

and transverse deflection shown in Fig. **2-3**, as follows:

At ξ=0:

$$\bar{V}_a = \bar{S}_a \bar{Y}(0) + (1 + F^2 s^2)\Theta(0) - (1 + D_G^2 s^2)\frac{d\bar{Y}(0)}{d\xi} \tag{2-22}$$

$$\bar{M}_a = -\frac{d\Theta(0)}{d\xi} \tag{2-23}$$

At ξ=1:

$$\bar{V}_b = \bar{S}_b \bar{Y}(1) - (1 + F^2 s^2)\Theta(1) + (1 + D_G^2 s^2)\frac{d\bar{Y}(1)}{d\xi} \tag{2-24}$$

$$\bar{M}_b = \frac{d\Theta(1)}{d\xi} \tag{2-25}$$

Likewise, the displacements and rotations at A and B are:

$$\bar{\Delta}_a = \bar{Y}(0) \tag{2-26}$$

$$\rho_a \Theta_a = \rho_a \Theta(0) + \frac{1 - \rho_a}{3}\bar{M}_a \tag{2-27}$$

$$\bar{\Delta}_b = \bar{Y}(1) \tag{2-28}$$

$$\rho_b \Theta_b = \rho_b \Theta(1) + \frac{1 - \rho_b}{3}\bar{M}_b \tag{2-29}$$

3. Differential transformation method (DTM)

The DTM is a mathematical technique first introduced by [27] to solve ordinary and partial differential equations (DE). This method, which is based on the Taylor series expansion, consists of expressing the solution in the form of a polynomial to obtain the analytical solution of the differential equation. This technique converts the DE into a recursive equation and the B.Cs. into a set of two linear algebraic equations [9]. Unlike other approaches available to solve DEs, the DTM provides a solution that is easy to follow and implement and allows to include the effects of multiple variables (i.e., generalized boundary conditions, soil inhomogeneity, variable cross-section, etc.) without adding any difficulty to the mathematical derivation [24]. Next, the transformation of the governing DE and corresponding B.Cs. of the pile segment proposed herein are presented.

3.1. Transformation of the governing DE

The lateral deformation of the element caused by the applied external forces and its rotation can be expressed respectively in terms of the DTM as follows:

$$J(\xi) = \bar{J}(0) + \bar{J}(1)\xi + \bar{J}(2)\xi^2 + ... + \bar{J}(m)\xi^m = \sum_{k=0}^{\infty} \bar{J}(k)\xi^k \tag{3-1}$$

$$\Theta(\xi) = \bar{\Theta}(0) + \bar{\Theta}(1)\xi + \bar{\Theta}(2)\xi^2 + ... + \bar{\Theta}(m)\xi^m = \sum_{k=0}^{\infty} \bar{\Theta}(k)\xi^k \tag{3-2}$$

where coefficients $\bar{J}(k)$ and $\bar{\Theta}(k)$ are found according to the Taylor series using:

$$\bar{J}(k) = \frac{1}{k!}\left[\frac{d^k Y(\xi)}{d\xi^k}\right]_{\xi=0} \tag{3-3}$$

$$\bar{\Theta}(k) = \frac{1}{k!}\left[\frac{d^k \Theta(\xi)}{d\xi^k}\right]_{\xi=0} \tag{3-4}$$

Table 3-1.: DTM properties [8, 7]

Original Function	**Transformed Function**
$Z(\xi) = Z_1(\xi) \pm Z_2(\xi)$	$\bar{Z}(k) = \bar{Z}_1(k) \pm \bar{Z}_2(k)$
$Z(\xi) = cZ_1(\xi)$	$\bar{Z}(k) = c\bar{Z}_1(k)$
$Z(\xi) = d^n Z_1(\xi)/d\xi^n$	$\bar{Z}(k) = ((k+n)!/k!)\bar{Z}_1(k+n)$
$Z(\xi) = Z_1(\xi) Z_2(\xi)$	$\bar{Z}(k) = \sum_{r=0}^{k} \bar{Z}_1(r) \bar{Z}_2(k-r)$
$Z(\xi) = \xi^n$	$\bar{Z}(k) = \delta(k-n) = \begin{cases} 0 & if \quad k \neq n \\ 1 & if \quad k = n \end{cases}$

Then, applying the properties of the DTM listed in Table **3-1**, the transformed equations of Eqs. (2-17) and (2-18) as follows:

$$\begin{aligned}
&\sum_{r=0}^{k} A_\xi (k-r)(r+1)\bar{\Theta}(r+1) + F^2 s^2 (k+1)\bar{\Theta}(r+1) \\
&+ \sum_{r=0}^{k} (k+1-r) A_\xi (k+1-r)\bar{\Theta}(r) - \sum_{r=0}^{k} A_\xi (k-r)(r+1)(r+2)\bar{J}(r+2) \\
&- D_G^2 s^2 (k+1)(k+2)\bar{J}(k+2) - \sum_{r=0}^{k} (k+1-r) A_\xi (k+1-r)(r+1)\bar{J}(r+1) \\
&+ s^2 \sum_{r=0}^{k} D_s (k-r)\bar{J}(k) - b^2 s^2 n \sum_{r=0}^{k} A_\xi (k-r)\bar{J}(r) + \frac{L}{A_{st}G}\bar{Q}(k) = 0
\end{aligned} \tag{3-5}$$

$$\begin{aligned}
&s^2 \sum_{r=0}^{k} I_\xi (k-r)(r+1)(r+2)\bar{\Theta}(r+2) + s^2 \sum_{r=0}^{k} (k+1-r) I_\xi (k-r+1)(r+1)\bar{\Theta}(r+1) \\
&- \sum_{r=0}^{k} A_\xi (k-r)\bar{\Theta}(r) - F^2 s^2 \bar{\Theta}(k) + b^2 s^2 R^2 \sum_{r=0}^{k} I_\xi (k-r)\bar{\Theta}(r) \\
&+ \sum_{r=0}^{k} A_\xi (k-r)(r+1)\bar{J}(r+1) + F^2 s^2 (k+1)\bar{J}(k+1) = 0
\end{aligned} \tag{3-6}$$

Using properties of table **3-1**, Eqs.(3-5) and (3-6) are rewritten as (see Appendix A. Transformed governing differential equation):

$$J(k+2) = \Bigg[(1+F^2s^2)(k+1)\bar{\Theta}(k+1) + 2(m-1)(k+1)\bar{\Theta}(k)$$
$$+ (m-1)^2(k+1)\bar{\Theta}(k-1) - 2(m-1)(k+1)^2 J(k+1)$$
$$+ \left(D_0^2 s^2 - (m-1)^2(k-1)(k) - b^2s^2n - 2(m-1)^2(k)\right) J(k)$$
$$+ \left(D_1^2 s^2 - 2b^2s^2n(m-1)\right) J(k-1) + \left(D_2^2 s^2 - b^2s^2n(m-1)^2\right) J(k-2)$$
$$+ \frac{L}{A_s(0)G}\bar{Q}(k) \Bigg] / \left((1+D_G^2 s^2)(k+1)(k+2)\right) \tag{3-7}$$

$$\bar{\Theta}(k+2) = \Bigg[-4s^2(m-1)(k+1)^2\bar{\Theta}(k+1)$$
$$+ \left(1 + F^2s^2 - b^2s^2R^2 - 6s^2(m-1)^2(k)(k+1)\right)\bar{\Theta}(k)$$
$$+ \left(2(m-1) - 4b^2s^2R^2(m-1) - 4s^2(m-1)^3(k-1)(k+1)\right)\bar{\Theta}(k-1)$$
$$+ \left((m-1)^2 - 6b^2s^2R^2(m-1)^2 - s^2(m-1)^4(k-2)(k+1)\right)\bar{\Theta}(k-2)$$
$$- 4b^2s^2R^2(m-1)^3\bar{\Theta}(k-3) - b^2s^2R^2(m-1)^4\bar{\Theta}(k-4) - (1+F^2s^2)(k+1)J(k+1)$$
$$- 2(m-1)(k)J(k) - (m-1)^2(k-1)J(k-1) \Bigg] / \left(s^2(k+1)(k+2)\right) \tag{3-8}$$

In this formulation, terms $\bar{J}(i)$ and $\bar{\Theta}(i)$ with $i < 0$ are equal to zero. Additionally, $I_\xi = ((1+(m-1)\xi)^4$, $A_\xi = ((1+(m-1)\xi)^2$. Coefficients $J(k+2)$ to $J(m)$ and $\bar{\Theta}(k+2)$ to $\bar{\Theta}(m)$ are calculated from Eqs. (3-7) and (3-8), except for $\bar{J}(0)$ to $\bar{J}(1)$ and $\bar{\Theta}(0)$ to $\bar{\Theta}(2)$. For a better understanding of the proposed methodology and how to operate with the recursive equation, the first four terms of the recursive equation are presented next.

For $k = 0$

$$J(2) = \Bigg[(1+F^2s^2)\bar{\Theta}(1) + 2(m-1)\bar{\Theta}(0) - 2(m-1)J(1) + \left(D_0^2 s^2 - b^2s^2n\right) J(0)$$
$$+ \frac{L}{A_s\,(0)\,G} r_1 \Bigg] / \left(2(1+D_G^2 s^2)\right) \tag{3-9}$$

$$\bar{\Theta}(2) = \Bigg[-4s^2(m-1)\bar{\Theta}(1) + (1+F^2s^2 - b^2s^2R^2)\bar{\Theta}(0) - (1+F^2s^2)J(1) \Bigg] /(2s^2) \tag{3-10}$$

For $k = 1$

$$J(3) = \Bigg[2(1+F^2s^2)\bar{\Theta}(2) + 4(m-1)\bar{\Theta}(1) + 2(m-1)^2\bar{\Theta}(0) \tag{3-11}$$
$$- 8(m-1)J(2) + \left(D_0^2 s^2 - b^2s^2n - 2(m-1)^2\right) J(1)$$
$$+ \left(D_1^2 s^2 - 2b^2s^2n(m-1)\right) J(0) + \frac{L^2}{A_s(0)G} s_1 \Bigg] / \left(6(1+D_G^2 s^2)\right) \tag{3-12}$$

$$\bar{\Theta}(3) = \Big[-16s^2(m-1)\bar{\Theta}(2) + \left(1 + F^2s^2 - b^2s^2R^2 - 12s^2(m-1)^2\right)\bar{\Theta}(1) + \left(2(m-1) - 4b^2s^2R^2(m-1)\right)\bar{\Theta}(0) - 2(1+F^2s^2)J(2) - 2(m-1)J(1) \Big] / (6s^2) \tag{3-13}$$

For $k = 2$

$$J(4) = \Big[3(1+F^2s^2)\bar{\Theta}(3) + 6(m-1)\bar{\Theta}(2) + 3(m-1)^2\bar{\Theta}(1) - 18(m-1)J(3) + (D_0^2s^2 - 2(m-1)^2 - b^2s^2n - 4(m-1)^2)J(2) + (D_1^2s^2 - 2b^2s^2n(m-1))J(1) + (D_2^2s^2 - b^2s^2n(m-1)^2)J(0) + \frac{L^3}{A_s(0)G}t_1 \Big] / \left(12(1+D_G^2s^2)\right) \tag{3-14}$$

$$\bar{\Theta}(4) = \Big[-36s^2(m-1)\bar{\Theta}(3) + \left(1 + F^2s^2 - b^2s^2R^2 - 36s^2(m-1)^2\right)\bar{\Theta}(2) + \left(2(m-1) - 4b^2s^2R^2(m-1) - 12s^2(m-1)^3\right)\bar{\Theta}(1) + \left((m-1)^2 - 6b^2s^2R^2(m-1)^2\right)\bar{\Theta}(0) - 3(1+F^2s^2)J(3) - 4(m-1)J(2) - (m-1)^2J(1) \Big] / (12s^2) \tag{3-15}$$

3.2. Stiffness Matrix Derivation

The solution of $J(\xi)$ and $\Theta(\xi)$ can be expressed as a polynomial in terms of $\bar{J}(0)$, $\bar{J}(1)$, $\bar{\Theta}(0)$ and $\bar{\Theta}(1)$ since the other coefficients depend on them. Thus, at $\xi = 1$, solutions can be conveniently rewritten as:

$$J(1) = \bar{J}(0)f_0 + \bar{J}(1)f_1 + \bar{\Theta}(0)f_2 + \bar{\Theta}(1)f_3 + f_p \tag{3-16}$$

$$\Theta(1) = \bar{J}(0)g_0 + \bar{J}(1)g_1 + \bar{\Theta}(0)g_2 + \bar{\Theta}(1)g_3 + g_p \tag{3-17}$$

where f_i, and g_i, are function that grouped the terms of the homogeneous solution of $J(\xi)$ and $\Theta(\xi)$ that are dependent on $\bar{J}(0)$, $\bar{J}(1)$, $\bar{\Theta}(0)$ and $\bar{\Theta}(1)$, respectively. For instance, coefficients f_0 and g_0 are determined by solving for $\bar{J}(\xi)$ and $\bar{\Theta}(\xi)$ when $\bar{J}(0) = 1$ and $\bar{J}(1) = \bar{\Theta}(0) = \bar{\Theta}(1) = Q(\xi) = 0$. f_1, f_2, f_3, g_1, g_2 and g_3 are found in a similar manner. f_p and g_p results from evaluating the terms of $\bar{J}(\xi)$ and $\bar{\Theta}(\xi)$ dependent on the particular solution.

Boundary conditions (Eqs. 2-22 to 2-25) can be transform as follow:

$$\bar{V}_a = \bar{S}_a\bar{J}(0) + (1+F^2s^2)\bar{\Theta}(0) - (1+D_G^2s^2)\bar{J}(1) \tag{3-18}$$

$$\bar{M}_a = -\bar{\Theta}(1) \tag{3-19}$$

$$\bar{V}_b = \bar{S}_b \bar{J}_{\xi=1} + (1 + F^2 s^2)\bar{\Theta}_{\xi=1} - (1 + D_G^2 s^2)\bar{J}'_{\xi=1} \tag{3-20}$$

$$\bar{M}_a = \bar{\Theta}_{\xi=1} \tag{3-21}$$

Eqs. (3-18) to (3-21) can be condensed in matrix form as follows:

$$\left\{\bar{M}\right\} = [S]\{C\} + \{J\} \tag{3-22}$$

where:

$$\left\{\bar{M}\right\} = \left\{\bar{V}_a \quad \bar{M}_a \quad \bar{V}_b \quad \bar{M}_b\right\}^T ; \{C\} = \left\{\bar{J}(0) \quad \bar{\Theta}(0) \quad \bar{J}(1) \quad \bar{\Theta}(1)\right\}^T$$

$$\{J\} = \begin{bmatrix} 0 \\ 0 \\ \bar{S}_b f_p - (1 + F^2 s^2) g_p + (1 + D_G^2 s^2) f'_p \\ g'_p \end{bmatrix}$$

$$[S] = \begin{bmatrix} \bar{S}_a & 1 + F^2 s^2 & -(1 + D_G^2 s^2) & 0 \\ 0 & 0 & 0 & -1 \\ S_{31} & S_{32} & S_{33} & S_{34} \\ g_0' & g_2' & g_1' & g_3' \end{bmatrix}$$

Coefficients of matrix $[S]$ are:

$$\begin{aligned} S_{31} &= \bar{S}_b f_0 - (1 + F^2 s2) g_0 + (1 + D_G^2 s^2) f_0' \\ S_{32} &= \bar{S}_b f_2 - (1 + F^2 s2) g_2 + (1 + D_G^2 s^2) f_2' \\ S_{33} &= \bar{S}_b f_1 - (1 + F^2 s2) g_1 + (1 + D_G^2 s^2) f_1' \\ S_{34} &= \bar{S}_b f_3 - (1 + F^2 s2) g_3 + (1 + D_G^2 s^2) f_3' \end{aligned} \tag{3-23}$$

Here, f_0' to f_3' represent the derivative of the functions f_0 and f_3 respectively. Subsequently, Eqs. (2-26) to (2-29) after applying transform the following expressions are found:

$$\bar{\Delta}_a = \bar{J}(0) \tag{3-24}$$

$$\rho_a \theta_a = \rho_a \bar{\Theta}(0) + \frac{1 - \rho_a}{3} \bar{M}_a \tag{3-25}$$

$$\bar{\Delta}_b = \bar{J}_{\xi=1} \tag{3-26}$$

$$\rho_b \theta_b = \rho_b \bar{\Theta}_{\xi=1} + \frac{1-\rho_b}{3} \bar{M}_b \tag{3-27}$$

In a similar manner, Eqs. (3-24) to (3-27) can be expressed in matrix form as follows:

$$[H]\{U\} = [Z]\{C\} + [B]\left\{\bar{M}\right\} + \{N\} \tag{3-28}$$

where:

$$[H] = \begin{bmatrix} 1 & 0 & 0 & 0 \\ 0 & \rho_a & 0 & 0 \\ 0 & 0 & 1 & 0 \\ 0 & 0 & 0 & \rho_b \end{bmatrix}; \{U\} = \begin{Bmatrix} \Delta_a \\ \theta_a \\ \Delta_b \\ \theta_b \end{Bmatrix}$$

$$[D] = \begin{bmatrix} 0 & 0 & 0 & 0 \\ 0 & \frac{1-\rho_a}{3} & 0 & 0 \\ 0 & 0 & 0 & 0 \\ 0 & 0 & 0 & \frac{1-\rho_b}{3} \end{bmatrix}; \{N\} = \begin{Bmatrix} 0 \\ 0 \\ f_p \\ \rho_b g_p \end{Bmatrix}$$

$$[Z] = \begin{bmatrix} 1 & 0 & 0 & 0 \\ 0 & \rho_a & 0 & 0 \\ f_0 & f_2 & f_1 & f_3 \\ \rho_b f_0 & \rho_b f_2 & \rho_b f_1 & \rho_b f_3 \end{bmatrix}$$

Then, from Eq. (3-22), $\{C\}$ can be found as:

$$\{C\} = [S]^{-1}\left\{\bar{M}\right\} - [S]^{-1}\{J\} \tag{3-29}$$

and substituting $\{C\}$ into Eq. (3-28), the vector of forces $\{M\}$ is:

$$\left\{\bar{M}\right\} = \left[ZS^{-1} + B\right]^{-1}[H]\{U\} + \left[ZS^{-1} + B\right]^{-1}\left\{ZS^{-1}J - N\right\} \tag{3-30}$$

3.3. Dynamic-stiffness matrix and load vector

The following reduced expression $\left\{\bar{M}\right\} = [ZS^{-1} + B]^{-1}[H]\{U\}$ is obtained when the transverse load is made zero [i.e. $q(x,t) = 0$] in Eq. (3-30), thus:

$$[K] = \left[ZS^{-1} + B\right]^{-1}[H] \tag{3-31}$$

Notice that the square matrix $[K]$ is the dynamic-stiffness matrix of the beam column AB shown in Fig. **2-1**, since it relates the vector of end moments and shears $\left\{\bar{M}\right\}$ with the vector of end rotation and displacements $\{U\}$.

The load vector of the member consist of the equivalent bending moments and transverse shears applied at the ends A and B such that the end rotations and displacements become zero. Thus, the load vector obtained from Eq. (3-30) making $\{U\} = \{0\}$ is as follows:

$$\{F_{EF}\} = \left[ZS^{-1} + B\right]^{-1} \left\{ZS^{-1}J - N\right\} \tag{3-32}$$

and Eq. (3-30) can be expressed as :

$$\left\{\bar{M}\right\} = [K]\{U\} + \{F_{EF}\} \tag{3-33}$$

In Eq. (3-33), it is important to note that it comprises two significant components: the homogeneous solution $[K]\{U\}$ and the particular solution $\{F_{EF}\}$. The complete solution for the beam-column depicted in Fig. **2-1** encompasses various influential factors. These factors include: (a) end axial load P, accounting for tension or compression at the beam-column ends; (b) uniformly distributed translational and rotational masses, considering both translational and rotational effects caused by distributed masses; (c) uniformly distributed two-parameter elastic foundation; (d) bending and shear deformations, accommodating the effects of deformations along the beam-column length; (e) generalized boundary conditions, considering flexural and transverse connections at the ends that impose significant boundary conditions; and (f) generalized transverse load, accounting for the influence of a generalized load acting on the beam-column. By considering all these factors, the complete solution provides a comprehensive understanding of the beam-column's behavior under different loading and boundary condition configurations.

3.4. Deflections, rotations, shear and bending moment along the member

Once the displacements corresponding to the free degrees of freedom and the reactions are known, the deflection $\bar{Y}(\xi)$, the total rotation $\Theta(\xi)$, the shear $V(\xi)$, and the bending moment $M(\xi)$ along the beam-column AB can be calculated directly as follows:

$$\bar{Y}(\xi) = \bar{J}(0)\,\xi^0 + \bar{J}(1)\,\xi^1 + \bar{J}(2)\,\xi^2 + \bar{J}(3)\,\xi^3 + \bar{J}(4)\,\xi^4 + ... + \bar{J}(m)\,\xi^m \tag{3-34}$$

$$\Theta(\xi) = \bar{\Theta}(0)\,\xi^0 + \bar{\Theta}(1)\,\xi^1 + \bar{\Theta}(2)\,\xi^2 + \bar{\Theta}(3)\,\xi^3 + \bar{\Theta}(4)\,\xi^4 + ... + \bar{\Theta}(m)\,\xi^m \tag{3-35}$$

$$\bar{V}(\xi) = A_s(\xi)G\left(\Theta(\xi) - \bar{Y}'(\xi)\right) + P\Theta(\xi) \tag{3-36}$$

$$\bar{M}(\xi) = EI(\xi)\,\Theta'(\xi) \tag{3-37}$$

3.4.1. Natural frequencies and buckling loads

In the context of free vibration analysis, the determination of the natural frequencies of the beam-column involves using Eq. (3-31) by equating the determinant of the dynamic-stiffness matrix to zero. On the other hand, when considering buckling loads, the critical axial load (P_{cr}) is obtained by setting the determinant of the dynamic-stiffness matrix of the structure (3-31) to zero at $\omega = 0$. These fundamental techniques play a crucial role in understanding the dynamic behavior and stability of the structure under different loading conditions.

4. Validation Examples

The proposed, simple analytical method is validated with six examples encompassing prismatic, tapered and stepped piles under partially or fully embedded conditions. The influence of the taper ratio (i.e., variation of the cross-sectional area and moment of inertia), distribution and magnitude of the modulus of sub-grade reaction and layer thickness ratio on the lateral response of piles in multi-layered soil is presented and discussed in detail where $p(x) = \kappa_s(x)y - \kappa_G y''(x)$ represents the Pasternak soil foundation, being κ_s the coefficient of sub-grade reaction in units of force/length^3 and κ_G units of force. The results from the proposed approach are compared with those obtained from SAP2000. Herein, the variation with depth of the radius, perimeter, diameter and second moment of inertia are computed, respectively, from Eqs. (2-1) to (2-4) [25].

4.1. Prismatic non-cylindrical element embedded in an homogeneous soil

To validate the model, one of the initial examples employed was a comparison with the method proposed by Arboleda Monsalve et al. [2]. In their firs example, a prismatic element with a square section and dimensions $A_g = 0{,}25\ m^2$; $A_s = 0{,}2075\ m^2$; $E = 12\ kN/mm^2$; $G = 5\ kN/mm^2$; $E = 12\ kN/mm^2$; $I = 5{,}208x10^9\ mm^4$; $\bar{m} = 6x10^{-7}\ Gg/mm$; $L = 6000\ mm$; $\rho_a = 0{,}7$; $\rho_b = 0{,}3$; $S_a = 15\ kN/mm$; $S_b = 25\ kN/mm$; $\kappa_s = 0{,}012\ kN/mm^2$; $\kappa_G = 0$ and $P = 3000\ kN$. From here, the variation of the moment at one of its ends is determined.

Fig. **4-1** presents the variation of the moment at point A with the frequency parameter b for the specific loading case of Example 1 [2]. The figure clearly demonstrates that the proposed model accurately captures the frequency variation, yielding results consistent with those presented by Arboleda Monsalve et al. [2]. It is worth noting that the value of Ma increases as the frequency of the applied load approaches any undamped natural frequency of the beam-column. When the resonance condition is reached, both the moment and force values tend towards infinity.

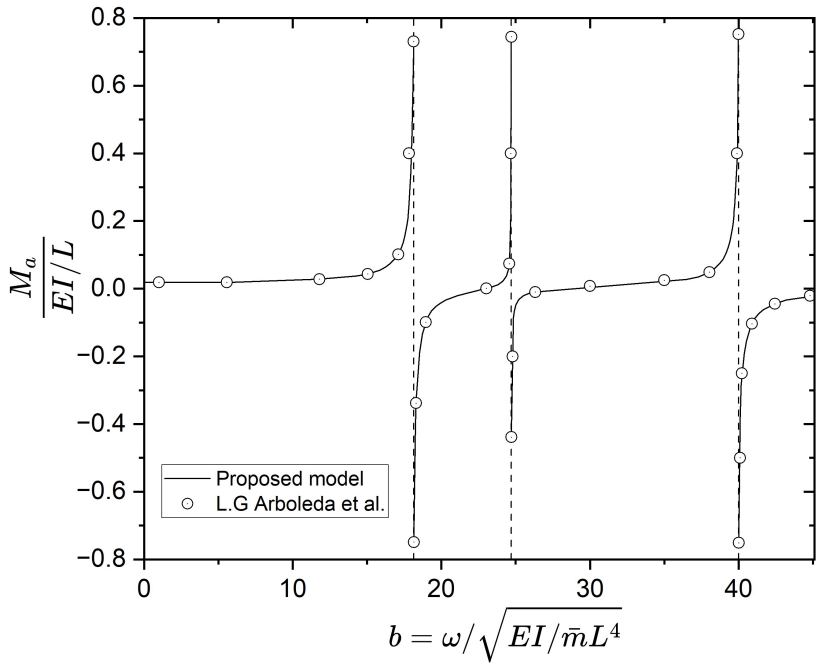

Figure 4-1.: Variation of moment at A with the frequency parameter b.

4.2. Transverse free vibration of axially loaded tapered friction piles in heterogeneous soil.

To verify the validity of the proposed formulation and the accuracy of solution method, the computed results are compared with the existing data in the literature. The first three natural frequencies of cylindrical end-bearing piles with Hinged-hinged end conditions are summarized in Table **4-1** as presented by Lee, J. K [12], where the solutions of Valsangkar and Pradhanang [22] using variable separating method; Karnovsky and Lebed [10] using the dynamic stiffness matrix method and Lee, J. K. using Runge-Kutta method combined with the determinant search technique are included for comparison.

Table 4-1.: Comparison of angular frequencies ω_i in rad/sec for cylindrical end-bearing piles ($r = 0{,}5\ m$, $L = 10\ m$, $k = 98\ kN/m^3$, $E = 20\ GPa$, $\rho = 2300\ kg/m^3$ and $P = 24\ MN$) [12].

Mode number	Valsangkar and Pradhanang [22]	Karnovsky and Lebed [10]	Jooh Kyu Lee and Su Han Park [12]	Present study
1	63.2	63.5	63.5	63.2
2	281.2	282	282	281.5
3	645.3	645.8	645.8	645.5

The results obtained from the proposed model showed good agreement with those from Valsangkar and Pradhanang [22], Karnovsky and Lebed [10], and Lee , J. K. [10]. The observed differences in the responses, considering the end condition and mode number, were found to be less than 0,61 %. This comparison confirms the reliability and effectiveness of the proposed model in predicting the behavior of non-uniform cylindrical end-bearing piles.

4.3. Fully-embedded hollow circular steel monopile embedded in an homogeneous soil

In order to validate the proposed model Fig. **4-2** presents the lateral deformation of a hollow circular steel monopile embedded in an homogeneous soil (i.e., $m_h = 0$) presented by Vega-Posada et al. [23] which assume a modulus of sub-grade reaction of $k_o = 0{,}04\ kN/mm^2$ and subjected, at its head, to a horizontal load of 3,000 kN. The following parameter are assumed for pile: $r = 2000\ mm$, $L = 10000\ mm$, $t = 46{,}35\ mm$, $E = 10k_0$, $v_p = 0{,}3$ (Poisson's ratio) and $G = 0{,}5E/(1 + v_p)$. The pile is free to rotate and move laterally at its top and bottom ends (i.e., $k_a = k_b = S_a = S_b = 0$).

Fig. **4-2**a to Fig. **4-2**d show the deflection, rotation, shear force and bending moment profiles. The analysis of a beam using Euler-Bernoulli theory and comparing it with Timoshenko theory reveals the importance of considering shear deformation. The inclusion of shear deformation significantly increases deflection and rotation at the pile head by factors of 1.59 and 2.85, respectively. Additionally, the Timoshenko beam model predicts higher bending moments, approximately 0.74 times those obtained from the Bernoulli beam model. The results from the proposed formulation align with previous findings by Vega-Posada et al. [23], emphasizing the significance of accounting for shear deformation in accurately predicting beam behavior. In summary, incorporating shear deformation in beam analysis, as supported by the Timoshenko theory, provides more accurate results than the traditional Bernoulli beam model.

4.4. Numerical applications for the tapered Timoshenko beam on two-parameter Pasternak foundations

To verify the convergence and accuracy of the proposed method, the first two dimensionless natural frequencies of a tapered Timoshenko beam with two-parameter Pasternak foundation are obtained for H-H boundary conditions with different taper ratios (m) and compared with previous results obtained by Zhang Jinlun [26]. In the following discussion, the variation of the dimensionless natural frequencies of free vibration under the previously defined dimensionless parameters is investigated. In order to show the significant contributions of

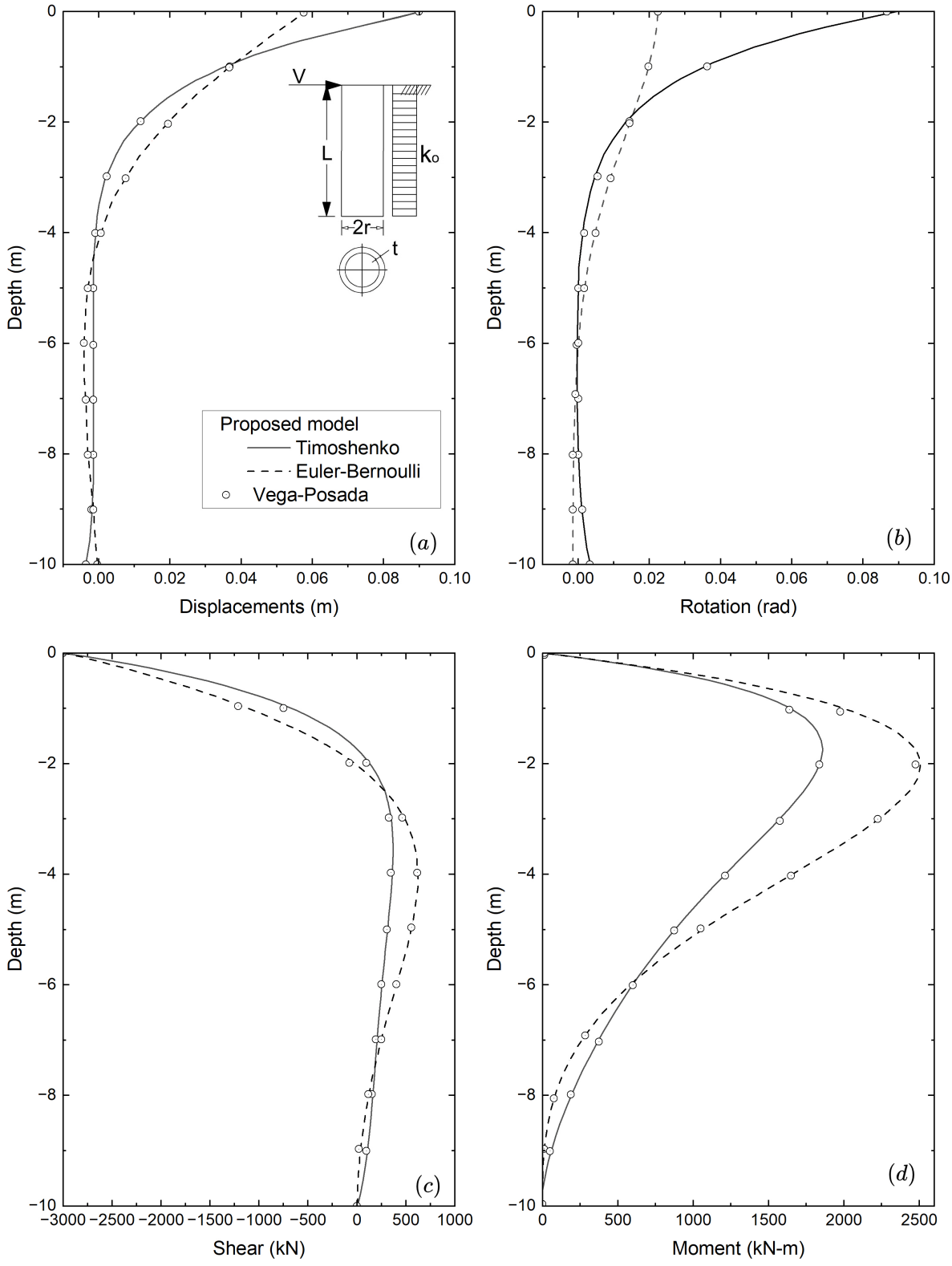

Figure 4-2.: Fully-embedded hollow circular steel mono-pile a) Displacements b) rotations c) shear and d) bending moment.

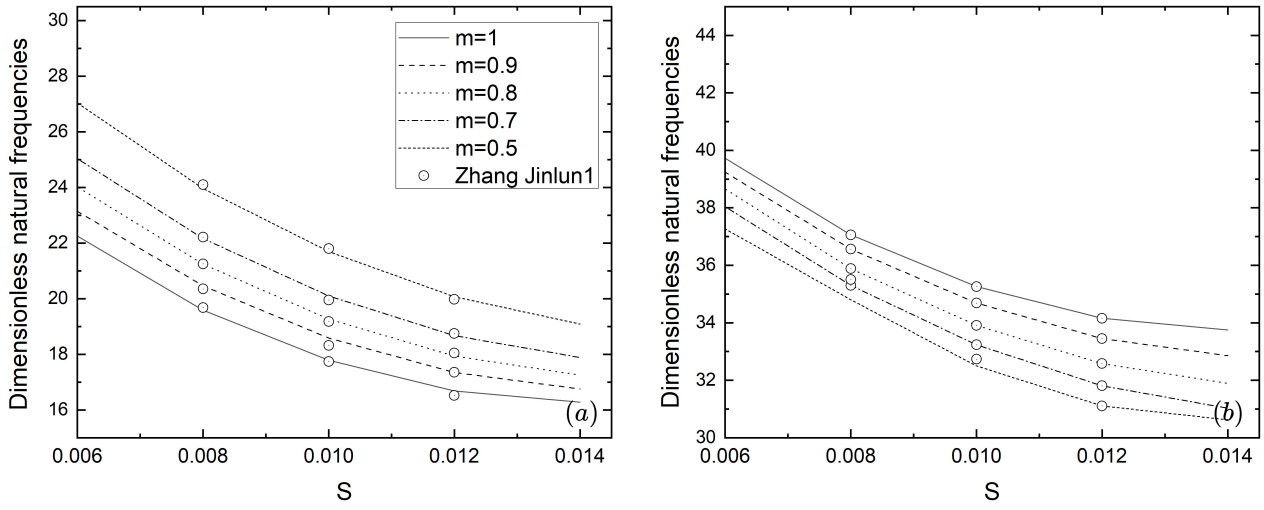

Figure 4-3.: First two dimensionless natural frequencies of a tapered Timoshenko beam with H-H boundary condition resting on two- parameter Pasternak foundations versus the dimensionless parameter s with different taper ratio. a) First natural frequency b) Second natural frequency.

the rotary inertia as well as the shear deformation, a reference has been established to $R = 0{,}0025$; referring to a beam, specifically a compact cylindrical pile, that encompasses the following distinct geometric characteristics: length 4 m, and diameter 0,8 m at the left end. Here, the Poisson's ratio is set as 0,2, the value range of the shear correction factor is set as $0{,}5 - 0{,}9$; the value range of s can be calculated by the previous parameters, and the parameters for the cross-section of the beam are $F = 0{,}25s; D_g = 2{,}5s$ and $D_s = 0{,}246s$.

The results, presented in Fig. **4-3**, reveal the influence of various parameters considered and their effects on the dimensionless natural frequencies of free vibration. Furthermore, the findings shows in align with previous research by Zhang Jinlun [26], validating the proposed method and its accuracy in predicting the beam's behavior. Fig. **4-3** specifically examines the impact of shear deformation on the natural frequencies. The study reveals a notable relationship between the taper ratio (m) and the natural frequencies of the beam. As the taper ratio decreases, the first natural frequency increases, while the second natural frequency shows the opposite trend. This highlights the influential role of the taper ratio in determining the beam's vibrational characteristics. Additionally, Zhang Jinlun [26] specifies that taper ratios below 0.5 are not recommended due to the potential occurrence of lateral buckling.

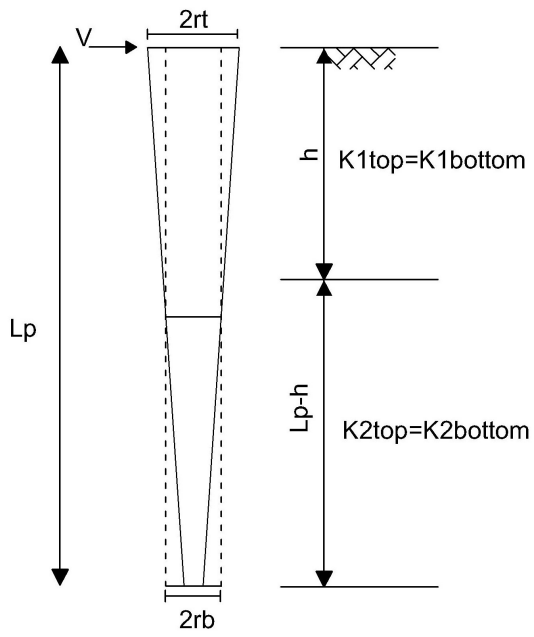

Figure 4-4.: Fully-embedded pile in a two-layer soil when subjected to a horizontal transverse load and bending moment.

4.5. Fully-embedded tapered pile in a two-layer homogeneous soil

Fig. **4-4** presents a tapered circular pile subjected to a lateral force or a bending moment at its head drawing parallels to the findings presented by Meza-Abalo et al. [14]. This analysis consider two taper ratios $m = 1$ (prismatic element) and $m = 0{,}8$. The top and bottom radios are calculated for each tapered ratio based on an equivalent radius $r_{eq} = 0{,}5$m located at $L_p/2$. It is assumed that the shear modulus, G_p, and pile length, L_p, are constant and equal to 8 GPa and 25 m, respectively. The pile under study is fully-embedded in a two-layer homogeneous soil ($\kappa_{s1t} = \kappa_{s1b}$ and $\kappa_{s2t} = \kappa_{s2b}$). Four stiffness ratios are studied. κ_{s1}/κ_{s2}=4 and κ_{s1}/κ_{s2}=2 correspond to an upper soil layer stiffer than the lower soil layer, meanwhile, κ_{s1}/κ_{s2}=0.5 and κ_{s1}/κ_{s2}=0.25 correspond to an upper soil layer softer than the lower soil layer. The thicknesses of the upper and lower layers are denoted by h and $L_p - h$, respectively. Thickness ratios ranging from h/L$_p$=0 (κ_2 as the only layer) to h/L$_p$=1 (κ_1 as the only layer) are considered in the analysis. Furthermore, it's worth noting that the modeling of this example was also performed using SAP2000 software.

The analysis of Fig. **4-5** reveals that the natural vibration frequencies are higher when the soil has a greater stiffness, indicated by $\kappa_{s1}/\kappa_{s2} < 1$ for h/L$_p$ < 0,2. Beyond this threshold, the frequency becomes independent of the soil stiffness, suggesting that a thicker upper layer

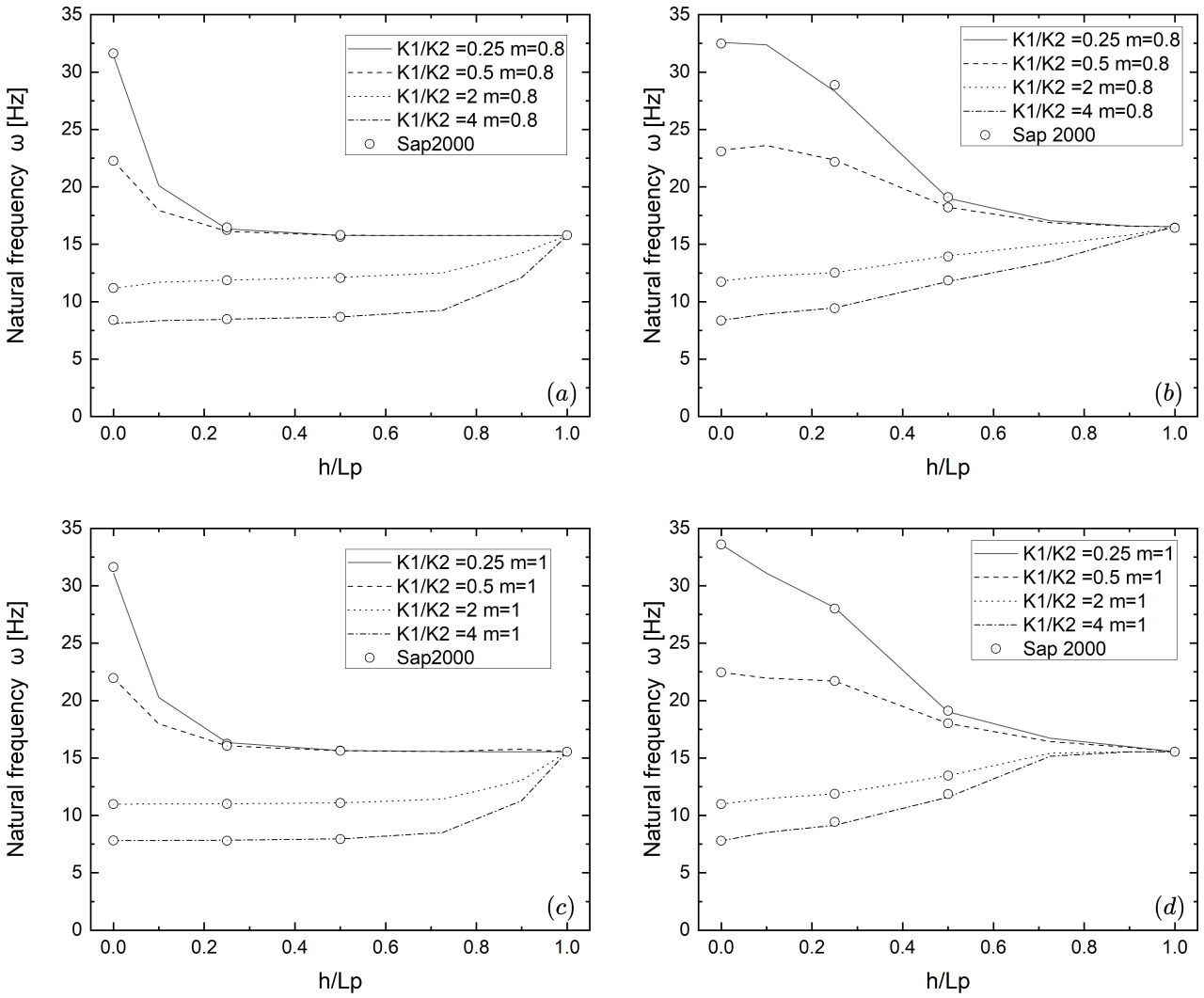

Figure 4-5.: Natural frequencies, a) first natural frequency for m=0.8, b) second natural frequency for m=0.8, c) first natural frequency for m=1, d) second natural frequency for m=1.

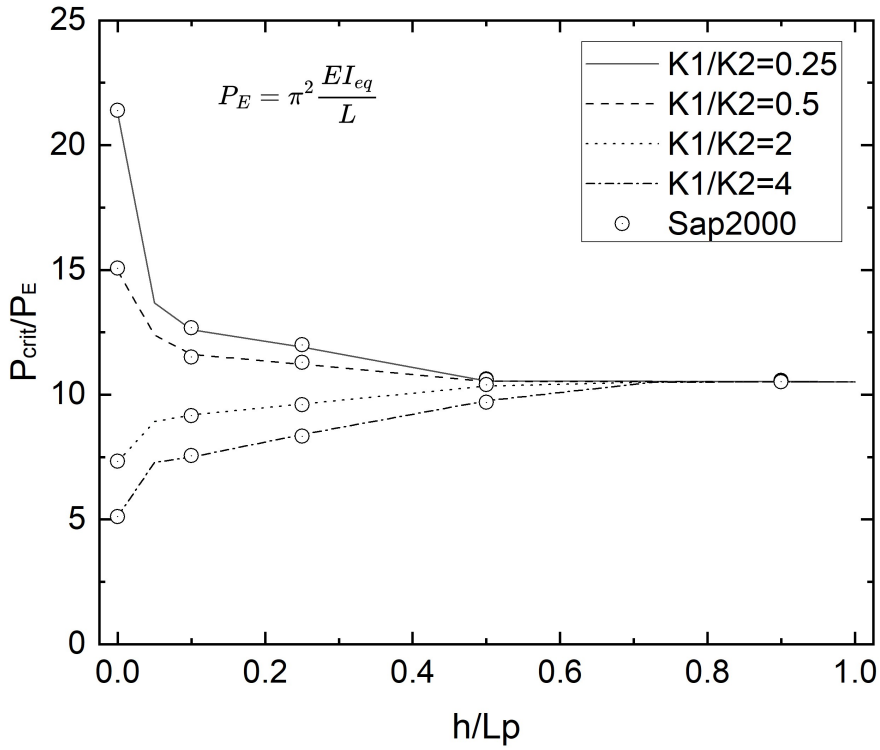

Figure 4-6.: Critical load for a cylindrical tapered pile embedded in two-layer homogeneous soil.

of less rigid soil does not necessarily decrease the frequency. Otherwise, in situations where the upper layer is stiffer than the lower layer ($\kappa_{s1}/\kappa_{s2} > 1$), the frequency increases slowly for $h/L_p < 0{,}6$. However, for higher values of this ratio, the frequency undergoes significant changes until reaching a point where the behavior is primarily influenced by the upper layer. Additionally, it is worth noting that when comparing prismatic beams to tapered beams, the behavior of natural frequencies varies depending on the soil conditions. When encountering stiffer soils ($\kappa_{s1}/\kappa_{s2} < 1$), the natural frequency remains consistent between the two beam types. However, in scenarios where the upper layer of soil is stiffer $\kappa_{s1}/\kappa_{s2} > 1$), a slight decrease in frequency values of approximately 7 % can be observed. It is important to highlight that when the ratio of the upper layer thickness to the prismatic beam length $h/L_p = 1$), the frequency values for both prismatic and tapered beams converge to the same value. This convergence suggests the presence of a single soil layer with a consistent stiffness value, denoted as κ_{s1}.

On the other hand, in Fig. **4-6**, the obtained results for the critical load calculation of the tapered beam case with $m = 0{,}8$ are shown. These results are normalized with respect to the Euler's critical load. In this analysis, it is assumed that the element is not laterally constrained. It can be observed that the increase in axial load capacity is dependent on

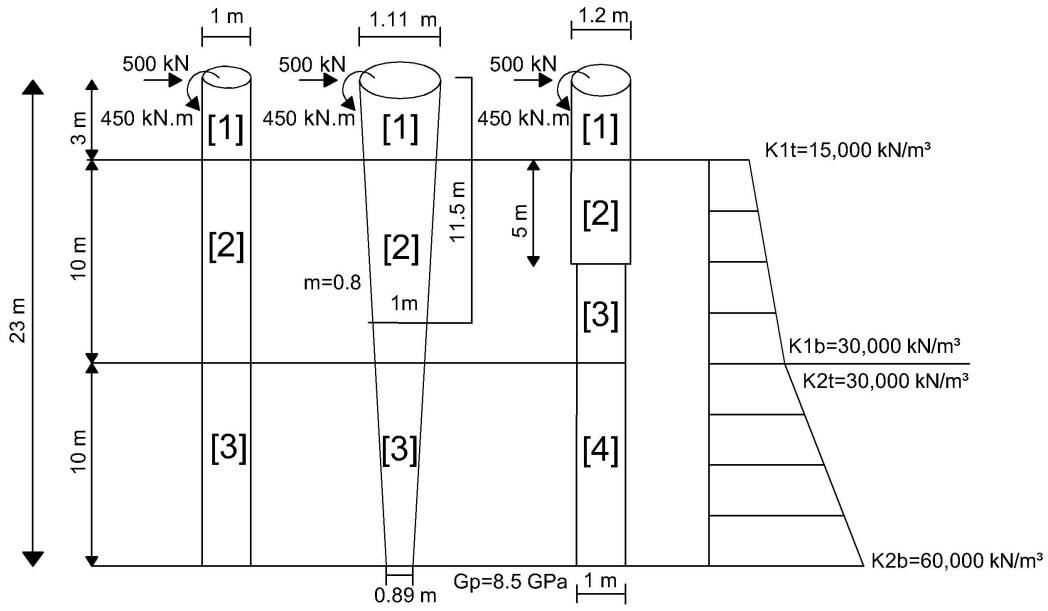

Figure 4-7.: Partially embedded (a) prismatic, (b) tapered and (c) stepped pile.

the soil stiffness for h/L_p ratios below 0.5. However, for higher ratios, the axial capacity is controlled by the upper layer and exhibits slight independence from variations in the stiffness of the lower layer. The results obtained from the proposed approach demonstrate an excellent agreement with FE software SAP2000. In it, each taper ratio necessitated a separate model, and the pile needed to be divided into 100 elements to accurately capture the cross-section variation and soil non-homogeneity, ensuring precise analysis.

4.6. Non-uniform circular piles partially embedded in a two-layer soil

This example serves as a demonstration of the proposed model's capability to accurately predict the first five frequencies of partially embedded piles in non-homogeneous soil. These predictions will be compared with the results obtained using SAP2000. The piles in this case have a total length of 23 m, with an unembedded portion of 3 m, and their properties are consistent with those utilized by Meza-Abalo et al. [14], for static case. The analysis is conducted for a prismatic, tapered and stepped pile (see Fig. **4-7**). The soil stratigraphy consists of two layers with a thickness of 10 m each. In both layers, the variation of the modulus of subgrade reaction follows a trapezoidal distribution with the following soil parameters assigned: (i) for layer 1, $\kappa_{s1t} = 15,000$ kN/m^3, $\kappa_{s1b} = 30,000$ kN/m^3 and $m_{h1} = 1,500$ kN/m^4 and (ii) for layer 2, $\kappa_{s2t} = 30,000$ kN/m^3, $\kappa_{s2b} = 60,000$ kN/m^3 and $m_{h2} = 3,000$ kN/m^4.

As shown in Figure **4-7**, both the prismatic and tapered piles are divided into three elements. Two elements represent the embedded portion, with one element assigned to each layer of soil, while the remaining element represents the unembedded portion. For the stepped pile, it is divided into four elements to accurately model the variation in the pile's cross-section within layer 1. To calculate the stiffness matrix of the unembedded portion, the relevant pile parameters are inputted, and the soil parameters are set to zero ($K_t = 0$, $K_b = 0$, and $m_h = 0$).

Fig. **4-8** shows the displacement, rotation, bending moment, and shear stress profiles along the three types of compared piles. It can be observed that the prismatic section exhibits higher deformations (displacement and rotation), indicating that, for piles with the same volume and length, non-prismatic sections perform better. Additionally, it is possible to notice that the obtained results match those found by Meza-Abalo [14].

The analysis obtain from Fig. **4-9** demonstrates that the first three vibration modes remain unaltered regardless of the beam's shape, given their equivalent volume and mass sections. However, noticeable variations are observed in the higher modes when comparing the tapered and stepped piles to the prismatic beam. Importantly , the results obtained for the partially embedded piles exhibit excellent agreement with those obtained from SAP2000, further validating the accuracy and reliability of the proposed model.

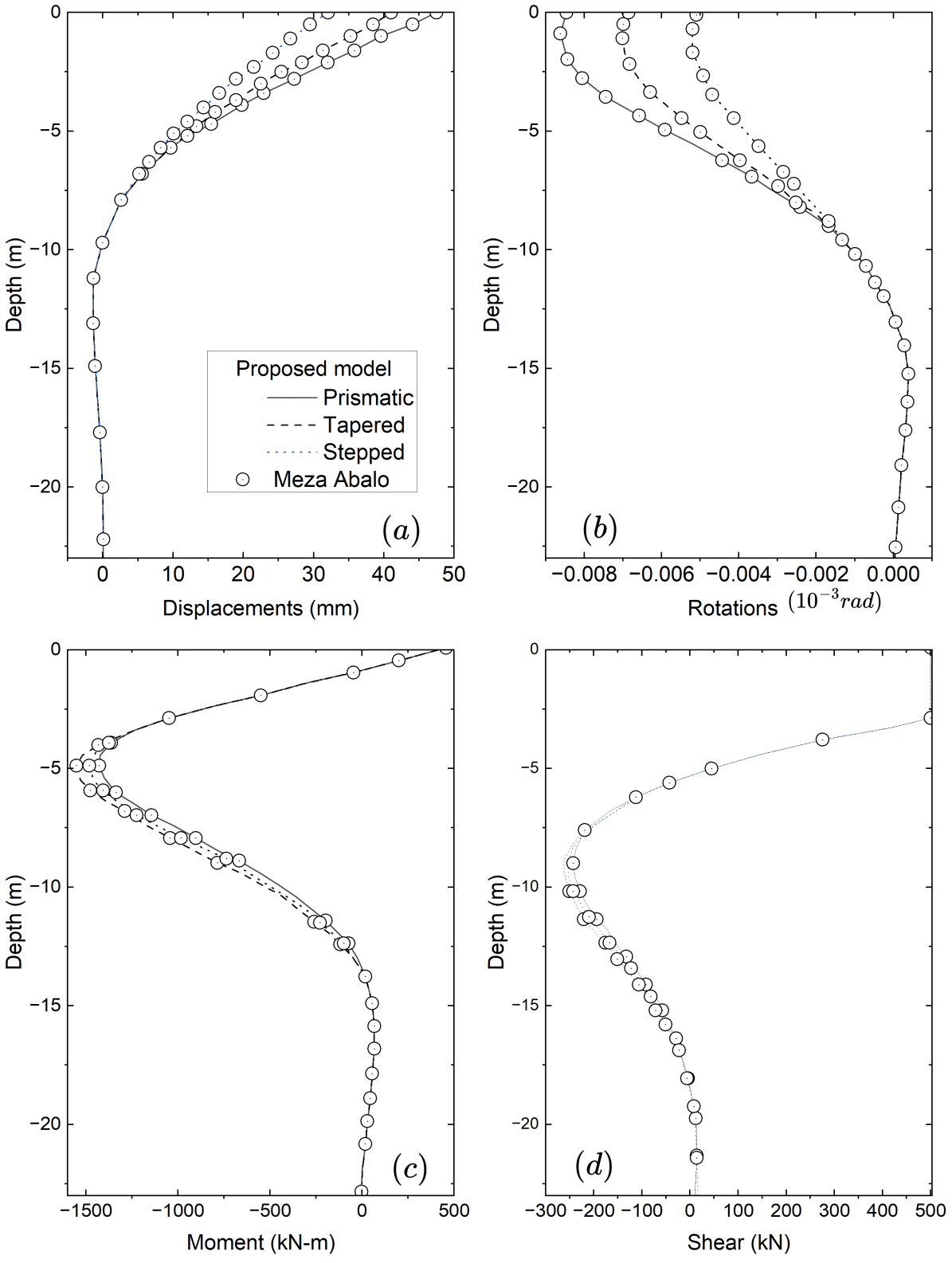

Figure 4-8.: (a) Lateral deformation, (b) rotation, (c) bending moment and (d) shear forces.

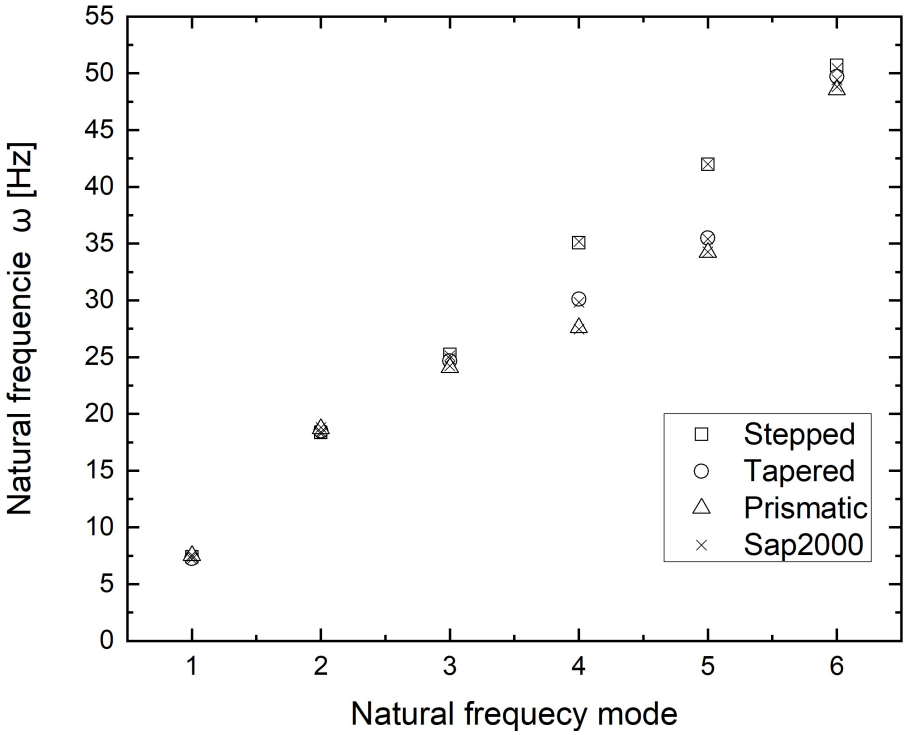

Figure 4-9.: Natural frequency modes of stepped, tapered and prismatic beams

5. Conclusions and recommendations

5.1. Conclusions

The developed analytical model offers a comprehensive framework for analyzing the static and dynamic behavior of Timoshenko tapered beams, specifically in the context of non-uniform cylindrical piles embedded in non-homogeneous soil. It incorporates a linear or trapezoidal distribution of the modulus of sub-grade reaction to account for soil in-homogeneity. The model allows for investigating lateral response in prismatic and variable cross-section piles, considering multi-layered soil conditions. Through four examples, the model examined the influence of parameters like embedded length, taper ratio, and soil inhomogeneity. The model's accuracy and reliability were validated by comparing results with other studies and established FE software like SAP2000, showing excellent agreement. This validates the model's capability to effectively capture the lateral response, natural frequency, and buckling loads of non-uniform partially or fully embedded piles in non-homogeneous multi-layered soil.

Based on this validation, the following additional conclusions can be drawn from this study:

- The proposed analytical model for analyzing of non-uniform cylindrical piles offers a practical and efficient solution derived using the Differential Transformation Method. It addresses the challenges posed by rigorous and complex analytical and numerical methodologies, providing a reliable and easy-to-implement tool for geotechnical practitioners.

- The proposed analytical model presents a significant advantage over SAP2000 in terms of computational efficiency. While SAP2000 requires multiple models and a high number of elements to accurately capture the response of a tapered pile with variable cross-sections and non-homogeneous soil, the proposed model achieves the same accuracy with a single element per soil layer or change in pile geometry. This results in a reduced computational cost and processing time. Additionally, the model's capability to account for soil inhomogeneity through the distribution of the modulus of subgrade reaction further enhances its applicability to real-world engineering problems involving non-uniform soil conditions.

- The model's ability to predict the lateral response, natural frequency, and buckling loads of non-uniform partially or fully embedded piles provides valuable insights for

optimizing pile design and ensuring structural stability in various soil conditions.

- The results obtained from the static analysis reveal that the buckling load capacity of the pile is influenced by the stiffness of the soil. The soil's stiffness provides confinement to the pile, thereby enhancing its performance in terms of axial load resistance. This finding emphasizes the significance of considering the soil properties and stiffness in designing piles to ensure their optimal load-bearing capacity. By incorporating soil stiffness into the analysis, engineers can effectively enhance the structural performance and stability of piles subjected to axial loads.

- The obtained results consistently indicate that in rigid soil conditions, the natural frequency of both prismatic and tapered beams remains similar. However, in soft soil conditions, the shape of the pile significantly influences the natural frequency. This finding highlights the importance of considering soil characteristics when analyzing the natural frequency of beams, particularly in scenarios involving soft soil conditions. By accounting for such factors, engineers can make more informed design decisions to ensure the desired performance of structures.

The developed analytical model efficiently analyzes Timoshenko tapered beams on non-homogeneous soil profiles. It utilizes the differential transform method to obtain closed-form solutions for free and forced vibrations, considering axial and transverse forces. The model's accuracy is validated by excellent agreement with previous research. This tool offers valuable insights into the dynamic behavior of non-uniform beams on non-homogeneous soil foundations, benefiting engineers and researchers in their analysis and design efforts. The analysis emphasizes the significance of the taper ratio in predicting natural frequencies and provides valuable information for optimizing the design of tapered Timoshenko beams.

5.2. Recommendations

In this thesis, the derivation of the stiffness matrix and load vector for an analytical solution addressing non-uniform cylindrical piles partially and fully embedded in non-homogeneous soils was successfully accomplished. However, there are several areas that could be further explored in future research:

- Evaluate the applicability of the proposed methodology to other sections of non-prismatic piles, broadening its scope and ensuring its versatility.

- Extend the formulation to account for dynamic loads on non-prismatic piles, such as those induced by wind, seismic activity, machinery, etc. This should involve considering soil degradation effects and conducting a thorough analysis of pile-soil dynamic interaction.

- Incorporate more sophisticated soil behavior models, such as non-linear or elasto-plastic models, to accurately capture the complex nature of soil response.
- Perform settlement analysis for step and tapered piles, varying parameters such as the number of steps, length, and taper ratios. It is crucial to validate the analysis by comparing the results with field testing data.

By addressing these aspects in future studies, a more comprehensive understanding of the behavior and performance of non-prismatic piles in different conditions can be achieved, further enhancing the practical applications of the research.

A. Appendix A: Transformed governing differential equation

Using the transformed functions listed in Table **3-1**, the terms of the governing differential equations can be transformed as follows:

$$\left(A_\xi + F^2 s^2\right) \frac{d\Theta}{d\xi} = \sum_{k=0}^{r} A_\xi \left(k-r\right)\left(r+1\right)\bar{\Theta}\left(r+1\right) + F^2 s^2 \left(k+1\right)\bar{\Theta}\left(r+1\right) \tag{A-1}$$

$$\sum_{k=0}^{r} A_\xi \left(k-r\right)\left(r+1\right)\bar{\Theta}\left(r+1\right) = \tag{A-2}$$
$$\sum_{k=0}^{r} \left[\delta\left(k-r\right) + 2(m-1)\delta\left(k-r-1\right) + (m-1)^2\delta\left(k-r-2\right)\right]\left(r+1\right)\bar{\Theta}\left(r+1\right)$$
$$= \left(k+1\right)\bar{\Theta}\left(k+1\right) + 2\left(m-1\right)\left(k\right)\bar{\Theta}\left(k\right) + \left(m-1\right)^2\left(k-1\right)\bar{\Theta}\left(k\right)$$

$$A_\xi^{'}\Theta = \sum_{k=0}^{r} \left(k+1-r\right) A_\xi \left(k-r+1\right)\bar{\Theta}\left(r\right) \tag{A-3}$$
$$= \sum_{k=0}^{r} \left(k-r+1\right)\left[\delta\left(k-r+1\right) + 2(m-1)\delta\left(k-r\right) + (m-1)^2\delta\left(k-r-1\right)\right]\bar{\Theta}\left(r\right)$$
$$= 2(m-1)\bar{\Theta}\left(k\right) + 2(m-1)^2\bar{\Theta}\left(k-1\right)$$

$$\left(A_\xi + D_G^2 s^2\right)\frac{d\bar{Y}^2}{d\xi^2} = \sum_{k=0}^{r} A_\xi\left(k-r\right)\left(r+1\right)\left(r+2\right)\bar{J}\left(r+2\right) + D_G^2 s^2\left(k+1\right)\left(k+2\right)\bar{J}\left(k+2\right) \tag{A-4}$$

$$\sum_{k=0}^{r} A_\xi\left(k-r\right)\left(r+1\right)\left(r+2\right)\bar{J}\left(r+2\right) \tag{A-5}$$
$$= \sum_{k=0}^{r}\left[\delta\left(k-r\right) + 2(m-1)\delta\left(k-r-1\right) + (m-1)^2\delta\left(k-r-2\right)\right]\left(r+1\right)\left(r+2\right)\bar{J}\left(r+2\right)$$
$$= \left(k+1\right)\left(k+2\right)\bar{J}\left(k+2\right) + 2(m-1)\left(k\right)\left(k+1\right)\bar{J}\left(k+1\right) + \left(m-1\right)^2\left(k-1\right)\left(k\right)\bar{J}\left(k\right)$$

$$A_{\xi}^{'}\frac{d\bar{Y}}{d\xi}=\sum_{k=0}^{r}\left(k-r+1\right)A_{\xi}\left(k-r+1\right)\left(r+1\right)\bar{J}\left(r+1\right) \tag{A-6}$$
$$=\sum_{k=0}^{r}\left(k-r+1\right)\left[\delta\left(k-r+1\right)+2(m-1)\delta\left(k-r\right)+(m-1)^{2}\delta\left(k-r-1\right)\right]\left(r+1\right)\bar{J}\left(r+1\right)$$
$$=2(m-1)\left(k+1\right)\bar{J}\left(k+1\right)+2(m-1)^{2}\left(k\right)\bar{J}\left(k\right)$$

$$\left(D_{s}^{2}s^{2}\left(\xi\right)-b^{2}s^{2}nA_{\xi}\right)\bar{Y}=s^{2}\sum_{k=0}^{r}D_{s}\left(k-r\right)\bar{J}\left(r\right)-b^{2}s^{2}n\sum_{k=0}^{r}A_{\xi}\left(k-r\right)\bar{J}\left(r\right) \tag{A-7}$$

$$s^{2}\sum_{k=0}^{r}D_{s}\left(k-r\right)\bar{J}\left(r\right) \tag{A-8}$$
$$=s^{2}\sum_{k=0}^{r}\left[D_{0}^{2}\delta\left(k-r\right)+D_{1}^{2}\delta\left(k-r-1\right)+D_{2}^{2}\delta\left(k-r-2\right)\right]\bar{J}\left(r\right)$$
$$=D_{0}^{2}s^{2}\bar{J}\left(k\right)+D_{1}^{2}s^{2}\bar{J}\left(k-1\right)+D_{0}^{2}s^{2}\bar{J}\left(k-2\right)$$

$$\left(D_{s}^{2}s^{2}\left(\xi\right)-b^{2}s^{2}nA_{\xi}\right)\bar{Y}=s^{2}\sum_{k=0}^{r}D_{s}\left(k-r\right)\bar{J}\left(r\right)-b^{2}s^{2}n\sum_{k=0}^{r}A_{\xi}\left(k-r\right)\bar{J}\left(r\right) \tag{A-9}$$

$$\frac{L}{A_{s}(0)G}Q\left(\xi\right)=\frac{L}{A_{s}(0)G}\bar{Q}\left(k\right)=\frac{L}{A_{s}(0)G}\left[r_{1}\delta\left(k\right)+s_{1}L\delta\left(k-1\right)+t_{1}L^{2}\delta\left(k-2\right)\right] \tag{A-10}$$

$$s^{2}I_{\xi}\frac{d^{2}\Theta}{d\xi^{2}}=s^{2}\sum_{k=0}^{m}I_{\xi}\left(k-r\right)\left(r+1\right)\left(r+2\right)\bar{\Theta}\left(r+2\right) \tag{A-11}$$
$$=s^{2}\sum_{k=0}^{r}\left[\,\delta\left(k-r\right)+4(m-1)\delta\left(k-r-1\right)+6(m-1)^{2}\delta\left(k-r-2\right)\right.$$
$$\left.+\,4(m-1)^{3}\delta\left(k-r-3\right)+(m-1)^{4}\delta\left(k-r-4\right)\,\right]\left(r+1\right)\left(r+2\right)\bar{\Theta}\left(r+2\right)$$
$$=s^{2}\left(k+1\right)\left(k+2\right)\bar{\Theta}\left(k+2\right)+4s^{2}(m-1)\left(k\right)\left(k+1\right)\bar{\Theta}\left(k+1\right)+6(m-1)^{2}s^{2}\left(k-1\right)\left(k\right)\bar{\Theta}\left(k\right)$$
$$+\,4(m-1)^{3}s^{2}\left(k-2\right)\left(k-1\right)\bar{\Theta}\left(k-1\right)+(m-1)^{4}s^{2}\left(k-3\right)\left(k-2\right)\bar{\Theta}\left(k-2\right)$$

$$s^2 I_\xi' \frac{d\Theta}{\xi} = s^2 \sum_{k=0}^{m} (k-r+1)\, I_\xi\,(k-r+1)\,(r+1)\,\bar{\Theta}\,(r+1) \tag{A-12}$$
$$= s^2 \sum_{k=0}^{r} (k-r+1)\,[\,\delta\,(k-r+1) + 4(m-1)\delta\,(k-r) + 6(m-1)^2\delta\,(k-r-1)$$
$$+ 4(m-1)^3\delta\,(k-r-2) + (m-1)^4\delta\,(k-r-3)\,]\,(r+1)\,\bar{\Theta}\,(r+1)$$
$$= 4s^2(m-1)\,(k+1)\,\bar{\Theta}\,(k+1) + 12(m-1)^2 s^2\,(k)\,\bar{\Theta}\,(k)$$
$$+ 12(m-1)^3 s^2\,(k-1)\,\bar{\Theta}\,(k-1) + 4(m-1)^4 s^2\,(k-2)\,\bar{\Theta}\,(k-2)$$

$$\left(A_\xi + F^2 s^2 - b^2 s^2 R^2 I_\xi\right)\Theta = \sum_{k=0}^{m} A_\xi\,(k-r)\,\bar{\Theta}\,(r) + F^2 s^2 \bar{\Theta}\,(k) - b^2 s^2 R^2 \sum_{k=0}^{m} I_\xi\,(k-r)\,\bar{\Theta}\,(r) \tag{A-13}$$

$$\sum_{k=0}^{r} A_\xi\,(k-r)\,\bar{\Theta}\,(r) = \tag{A-14}$$
$$\sum_{k=0}^{r} \left[\delta\,(k-r) + 2(m-1)\delta\,(k-r-1) + (m-1)^2\delta\,(k-r-2)\right]\bar{\Theta}\,(r)$$
$$= \bar{\Theta}\,(k) + 2\,(m-1)\,\bar{\Theta}\,(k-1) + (m-1)^2\,\bar{\Theta}\,(k-2)$$

$$b^2 s^2 R^2 \sum_{k=0}^{m} I_\xi\,(k-r)\,\bar{\Theta}\,(r) \tag{A-15}$$
$$= b^2 s^2 R^2 \sum_{k=0}^{r} [\,\delta\,(k-r) + 4(m-1)\delta\,(k-r-1) + 6(m-1)^2\delta\,(k-r-2)$$
$$+ 4(m-1)^3\delta\,(k-r-3) + (m-1)^4\delta\,(k-r-4)\,]\,\bar{\Theta}\,(r)$$
$$= b^2 s^2 R^2 \left(\bar{\Theta}\,(k) + 4(m-1)\bar{\Theta}\,(k-1) + 6(m-1)^2\,(k)\,\bar{\Theta}\,(k-2)\right.$$
$$\left. + 4(m-1)^3\bar{\Theta}\,(k-3) + (m-1)^4\bar{\Theta}\,(k-4)\right)$$

$$\left(A_\xi + F^2 s^2\right)\frac{d\bar{Y}}{d\xi} = \sum_{k=0}^{r} A_\xi\,(k-r)\,(r+1)\,\bar{J}\,(r+1) + F^2 s^2\,(k+1)\,\bar{J}\,(k+1) \tag{A-16}$$

$$\sum_{k=0}^{r} A_{\xi}\left(k-r\right)\left(r+1\right)\bar{J}\left(r+1\right) \tag{A-17}$$

$$= \sum_{k=0}^{r}\left[\delta\left(k-r\right)+2(m-1)\delta\left(k-r-1\right)+(m-1)^{2}\delta\left(k-r-2\right)\right]\left(r+1\right)\bar{J}\left(r+1\right)$$

$$= \left(k+1\right)\bar{J}\left(k+1\right)+2\left(m-1\right)\left(k\right)\bar{J}\left(k\right)+\left(m-1\right)^{2}\left(k-1\right)\bar{J}\left(k-1\right)$$

Bibliografía

[1] Al-Gahtani, Husain J.: Exact stiffnesses for tapered members. En: *Journal of structural Engineering* 122 (1996), Nr. 10, p. 1234–1239

[2] Arboleda-Monsalve, Luis G. ; Zapata-Medina, David G. ; Aristizabal-Ochoa, J D.: Timoshenko beam-column with generalized end conditions on elastic foundation: Dynamic-stiffness matrix and load vector. En: *Journal of Sound and Vibration* 310 (2008), Nr. 4-5, p. 1057–1079

[3] Aristizabal-Ochoa, J D.: First-and second-order stiffness matrices and load vector of beam-columns with semirigid connections. En: *Journal of Structural Engineering* 123 (1997), Nr. 5, p. 669–678

[4] Aristizabal-Ochoa, J D.: Timoshenko beam-column with generalized end conditions and nonclassical modes of vibration of shear beams. En: *Journal of engineering mechanics* 130 (2004), Nr. 10, p. 1151–1159

[5] Cheng, Franklin Y.: Vibrations of Timoshenko beams and frameworks. En: *Journal of the structural division* 96 (1970), Nr. 3, p. 551–571

[6] Cheng, Franklin Y. ; Pantelides, Chris P.: Dynamic Timoshenko beam-columns on elastic media. En: *Journal of Structural Engineering* 114 (1988), Nr. 7, p. 1524–1550

[7] Hassan, IH Abdel-Halim: Application to differential transformation method for solving systems of differential equations. En: *Applied Mathematical Modelling* 32 (2008), Nr. 12, p. 2552–2559

[8] Ho, Shing H. ; Chen, Cha'o K.: Analysis of general elastically end restrained non-uniform beams using differential transform. En: *Applied Mathematical Modelling* 22 (1998), 4, Nr. 4-5, p. 219–234. – ISSN 0307–904X

[9] Jang, Ming-Jyi ; Chen, Chieh-Li: Analysis of the response of a strongly nonlinear damped system using a differential transformation technique. En: *Applied Mathematics and Computation* 88 (1997), Nr. 2-3, p. 137–151

[10] Karnovsky, IA ; Lebed, OI. *Formulas for structural dynamics, 2004*

[11] Khan, M K. ; El Naggar, M H. ; Elkasabgy, Mohamed: Compression testing and analysis of drilled concrete tapered piles in cohesive-frictional soil. En: *Canadian Geotechnical Journal* 45 (2008), Nr. 3, p. 377–392

[12] Lee, Joon K. ; Park, Su H. ; Kim, Youngho: Transverse free vibration of axially loaded tapered friction piles in heterogeneous soil. En: *Soil Dynamics and Earthquake Engineering* 117 (2019), 02, p. 116–121

[13] Manandhar, Suman ; Yasufuku, Noriyuki ; Omine, Kiyoshi ; Kobayashi, Taizo: Response of tapered piles in cohesionless soil based on model tests. En: *Journal of Nepal Geological Society* 40 (2010), p. 85–92

[14] Meza Abalo, Maria de los Angeles C.: *Analytical solution for the soil-structure interaction of a non-uniform section pile on non-homogeneous soil conditions*, Universidad Nacional de Colombia, Tesis de Grado, 2022

[15] Palacio-Betancur, Alejandro ; Aristizabal-Ochoa, J D.: Statics, stability and vibration of non-prismatic linear beam-columns with semirigid connections on elastic foundation. En: *Engineering Structures* 181 (2019), p. 89–94

[16] Reese, Lymon C. ; Isenhower, William M. ; Wang, Shin-Tower: *Analysis and design of shallow and deep foundations*. Vol. 10. John Wiley & Sons, 2005

[17] Robinsky, E I. ; Sagar, W L. ; Morrison, C F.: Effect of Shape and Volume on the Capacity of Model Piles in Sand. En: *Canadian Geotechnical Journal* 1 (1964), Nr. 4, p. 189–204

[18] Sowers, George B. ; Sowers, George F.: *Introductory soil mechanics and foundations*. LWW, 1951

[19] Timošenko, Stepan P. ; Gere, James M.: *Theory of elastic stability*. McGraw-Hill, 1961

[20] Timoshenko, Stephan P.: X. On the transverse vibrations of bars of uniform cross-section. En: *The London, Edinburgh, and Dublin Philosophical Magazine and Journal of Science* 43 (1922), Nr. 253, p. 125–131

[21] Timoshenko, Stephen P.: LXVI. On the correction for shear of the differential equation for transverse vibrations of prismatic bars. En: *The London, Edinburgh, and Dublin Philosophical Magazine and Journal of Science* 41 (1921), Nr. 245, p. 744–746

[22] Valsangkar, AJ ; Pradhanang, RB: Free vibration of partially supported piles. En: *Journal of engineering mechanics* 113 (1987), Nr. 8, p. 1244–1247

[23] Vega-Posada, Carlos A.: Analytical Formulation for the Study of the Effect of Shear Deformations on Beam-Columns and Piles: Engesser and Haringx theories. En: *under review and pending approval* (2023)

[24] Vega-Posada, Carlos A. ; Gallant, Aaron P. ; Areiza-Hurtado, Mauricio: Simple approach for analysis of beam-column elements on homogeneous and non-homogeneous elastic soil. En: *Engineering Structures* 221 (2020), p. 111110

[25] Vega-Posada, Carlos A. ; Gallant, Aaron P. ; Carvajal-Muñoz, J S.: Simplified analytical method for static and stability analysis of circular tapered friction piles. En: *Engineering Structures* 251 (2022), p. 113498

[26] Zhang, Ling ; Zhao, Minghua ; Zou, Xinjun: Behavior of laterally loaded piles in multilayered soils. En: *International Journal of Geomechanics* 15 (2015), Nr. 2, p. 06014017

[27] Zhou, J. K.: Differential transformation and its applications for electrical circuits. En: *Huarjung Univ. Press.* (1986)